SMALL SCALE PROPERTIES IN THE MARINE BOUNDARY LAYER

Theron Carl Bone

NAVAL POSTGRADUATE SCHOOL
Monterey, California

THESIS

SMALL SCALE PROPERTIES IN THE

MARINE BOUNDARY LAYER

by

Theron Carl Bone

September 1974

Thesis Advisor: K. L. Davidson

SECURITY CLASSIFICATION OF THIS PAGE (When Data Entered)

REPORT DOCUMENTATION PAGE

READ INSTRUCTIONS BEFORE COMPLETING FORM

1. REPORT NUMBER	2. GOVT ACCESSION NO. / 3. RECIPIENT'S CATALOG NUMBER
4. TITLE (and Subtitle): Small Scale Properties in the Marine Boundary Layer	5. TYPE OF REPORT & PERIOD COVERED: Master's Thesis, September 1974
	6. PERFORMING ORG. REPORT NUMBER
7. AUTHOR(s): Theron Carl Bone	8. CONTRACT OR GRANT NUMBER(s)
9. PERFORMING ORGANIZATION NAME AND ADDRESS: Naval Postgraduate School, Monterey, California 93940	10. PROGRAM ELEMENT, PROJECT, TASK AREA & WORK UNIT NUMBERS
11. CONTROLLING OFFICE NAME AND ADDRESS: Naval Postgraduate School, Monterey, California 93940	12. REPORT DATE: September 1974
	13. NUMBER OF PAGES: 70
14. MONITORING AGENCY NAME & ADDRESS (if different from Controlling Office): Naval Postgraduate School, Monterey, California 93940	15. SECURITY CLASS. (of this report): Unclassified
	15a. DECLASSIFICATION/DOWNGRADING SCHEDULE

16. DISTRIBUTION STATEMENT (of this Report)

Approved for public release; distribution unlimited.

17. DISTRIBUTION STATEMENT (of the abstract entered in Block 20, if different from Report)

18. SUPPLEMENTARY NOTES

19. KEY WORDS (Continue on reverse side if necessary and identify by block number)

20. ABSTRACT (Continue on reverse side if necessary and identify by block number)

Fluctuating velocity and temperature data collected from instruments mounted at three levels on the R/V ACANIA were analyzed. The structure of atmospheric turbulence was examined on the basis of spectral distributions of wind and temperature fluctuations over the ocean. The results of this study were utilized to determine the validity of present formulations and prediction techniques for the momentum flux and the temperature-structure parameter over water.

DD FORM 1 JAN 73 1473 EDITION OF 1 NOV 65 IS OBSOLETE
S/N 0102-014-6601 |
(Page 1)

SECURITY CLASSIFICATION OF THIS PAGE (When Data Entered)

For the stability conditions encountered, the momentum flux calculations support present expressions for the constant flux layer. Proper directional deviation from prediction of the variation of ε with height was observed. When corrections for stability were applied, proper adjustment toward the predictions were noted. However, complete adjustment was not evident. This suggests other factors as wind wave effects may be important. C_T^2 calculations were in agreement with present formulations and prediction techniques.

Small Scale Properties in the Marine Boundary Layer

by

Theron Carl Bone
Lieutenant, United States Navy
B.S., Oregon State University, 1967

Submitted in partial fulfillment of the
requirements for the degree of

MASTER OF SCIENCE IN METEOROLOGY

from the

NAVAL POSTGRADUATE SCHOOL
September 1974

ABSTRACT

Fluctuating velocity and temperature data collected from instruments mounted at three levels on the R/V ACANIA were analyzed. The structure of atmospheric turbulence was examined on the basis of spectral distributions of wind and temperature fluctuations over the ocean. The results of this study were utilized to determine the validity of present formulations and prediction techniques for the momentum flux and the temperature-structure parameter over water.

For the stability conditions encountered, the momentum flux calculations support present expressions for the constant flux layer. Proper directional deviation from prediction of the variation of ε with height was observed. When corrections for stability were applied, proper adjustment toward the predictions were noted. However, complete adjustment was not evident. This suggests other factors as wind wave effects may be important. C_T^2 calculations were in agreement with present formulations and prediction techniques.

TABLE OF CONTENTS

I. INTRODUCTION - 11

II. THEORETICAL CONSIDERATIONS - - - - - - - - - - - - - - - - - 14

A. THE TEMPERATURE-STRUCTURE PARAMETER- - - - - - - - - - - - 14

B. BALANCE EXPRESSION FOR TURBULENT KINETIC ENERGY - 17

C. VARIATION OF ε WITH HEIGHT - - - - - - - - - - - - - - - 19

D. VARIATION OF C_T^2 WITH HEIGHT - - - - - - - - - - - - - - 20

E. KOLMOGOROV'S SPECTRAL SIMILARITY EXPRESSIONS - - - - - - - 22

III. OBSERVATIONS - 27

A. DATA COLLECTION- 27

B. EQUIPMENT- 27

1. Fluctuating Velocity and Temperature Measurements - 27

2. Mean Velocity, Temperature and Humidity Measurements- - - - - - - - - - - - - - - - - - 27

C. CALIBRATION- 29

1. Calibration of Hot Wire Sensors- - - - - - - - - - - - - 29

2. Calibration of Platinum Wire Sensors - - - - - - - - - 32

IV. DATA REDUCTION AND ANALYSIS- - - - - - - - - - - - - - - - - 36

A. PRELIMINARY ANALYSIS - - - - - - - - - - - - - - - - - - - 36

B. DIGITAL METHODS- 36

1. Analog to Digital Conversion - - - - - - - - - - - - - 36

2. Seven Track to Nine Track Conversion - - - - - - - - - 36

3. Digital Analysis Programs- - - - - - - - - - - - - - - 38

C. SCALING PROCEDURES - 38

V. INTERPRETATION OF SPECTRA - 42

A. SINGLE POINT METHOD - - - - - - - - - - - - - - - - - - - 42

B. INTERCEPT METHOD- 42

1. Determination of ε - - - - - - - - - - - - - - - - - 42

2. Determination of C_T^2 - - - - - - - - - - - - - - - - - 43

C. INNER SCALE METHOD- 43

VI. RESULTS - 46

A. SUMMARY OF PERIODS EXAMINED - - - - - - - - - - - - - - - 46

B. VELOCITY RESULTS- 46

C. TEMPERATURE RESULTS - - - - - - - - - - - - - - - - - - - 56

VII. CONCLUSIONS AND RECOMMENDATIONS - - - - - - - - - - - - - - - 66

LIST OF REFERENCES- 68

INITIAL DISTRIBUTION LIST - 69

LIST OF TABLES

I. Data Periods Considered in this Study - - - - - - - - - - - - - 47

II. ε and Momentum Flux Calculations using the Intercept Method- 48

III. C_T^2 Calculations using the Intercept Method- - - - - - - - - 58

LIST OF FIGURES

1. The R/V ACANIA operated by the Department of Oceanography - 12

2. The dimensionless temperature-structure parameter versus Richardson number - 16

3. An illustration of the effect of stability on the variation of ε with height - - - - - - - - - - - - - - - - - - 21

4. An illustration of the effect of stability on the variation of C_T^2 with height - - - - - - - - - - - - - - - - - - 23

5. A schematic drawing showing spectral transfer and illustrating (A) energy containing region (B) inertial subrange (C) dissipation range and (D) universal equilibrium range - 25

6. Mounting arrangements- 28

7. Picture showing equipment used aboard R/V ACANIA to obtain fluctuating velocity and temperature data- - - - - - 30

8. Picture showing equipment used aboard R/V ACANIA to obtain mean velocity and temperature data - - - - - - - - - 31

9. Hot wire calibration plot- - - - - - - - - - - - - - - - - - 33

10. Platinum wire transfer function plot - - - - - - - - - - - - - 35

11. Typical velocity and temperature signals - - - - - - - - - - - 37

12. SCOR spectral statistics - - - - - - - - - - - - - - - - - - 39

13. SCOR spectral plot - 40

14. Intercept plot for velocity data - - - - - - - - - - - - - - - 44

15. Intercept plot for temperature data- - - - - - - - - - - - - - 45

16. Velocity spectrum level 1 for 1855-1913, 18 Jan 74 - - - - - - 50

17. Velocity spectrum level 2 for 1855-1913, 18 Jan 74 - - - - - - 51

18. Velocity spectrum level 3 for 1855-1913, 18 Jan 74 - - - - - - 52

19. Measured values of ε vs height for 1834-1854
18 Jan 74- 53

20. Measured values of ε vs height for 1855-1913
18 Jan 74- 54

21. Measured values of ε vs height for 1914-1932
18 Jan 74- 55

22. Temperature spectrum level 1 for 1855-1913
18 Jan 74- 59

23. Differential temperature spectrum for fluctuating temperature data separated by r = 10 cm, level 2 for 1855-1913, 18 Jan 74 - - - - - - - - - - - - - - - - - - - 60

24. Temperature spectrum level 3 for 1855-1913
18 Jan 74- 61

25. Measured values of C_T^2 vs height for 1834-1854
18 Jan 74- 62

26. Measured values of C_T^2 vs height for 1855-1913
18 Jan 74- 63

27. Measured values of C_T^2 vs height for 1914-1932
18 Jan 74- 64

ACKNOWLEDGEMENTS

I would like to express my gratitude and appreciation to Dr. Kenneth L. Davidson who gave his time, his knowledge, and his experience to aid in the completion of this research. Special thanks to Dr. Thomas Houlihan for his advice in the utilization and calibration of electronic equipment used in this study. I would also like to acknowledge Professor Charles L. Taylor for contributing photographs used in this study and Mr. Steve Rinard for his assistance in equipment and experiment preparation.

To my wife Diane, who gave moral support by her concern, patience and understanding, my renewed affection.

I. INTRODUCTION

Interdisciplinary investigations are being conducted at the Naval Postgraduate School to correlate optical propagation and atmospheric turbulence data in the marine boundary layer. Such information is necessary for design of future naval systems. In these investigations, personnel from the Meteorology, Mechanical Engineering, Oceanography, and Physics departments have been obtaining shipboard observational data to evaluate optical propagation in the near-ocean environment.

The purpose of this study is to examine the structure of atmospheric turbulence on the basis of spectral distributions of wind and temperature fluctuations. Turbulence similarity expressions have been tested primarily over land. Only a few over water results have been obtained. Observational results from this study will provide a basis on which to evaluate and improve existing techniques in predicting over water optical propagation.

During January 1974, an observational experiment was made aboard the Naval Postgraduate School research vessel, R/V ACANIA shown in Figure 1. This experiment was conducted in Monterey Bay approximately two miles offshore. The experimental location provided the near-ocean environment for turbulence data collection as well as the platform for ship to shore optical propagation data collection. Meteorological measurements of wind and temperature were conducted at three levels.

The scope of this study concerned the examination of the turbulent fluctuations of velocity and temperature in the marine environment.

Figure 1. The R/V ACANIA

The examination included an evaluation of the height variation in the constant flux layer of (1) ε (the viscous dissipation of turbulent kinetic energy) and (2) C_T^2 (the temperature structure parameter).

II. THEORETICAL CONSIDERATIONS

A. THE TEMPERATURE-STRUCTURE PARAMETER

An important parameter in describing optical propagation is the refractive-index-structure parameter, C_N^2 . According to Wyngaard, et al (1971), C_N^2 can be related to its counter part, the temperature-structure parameter, C_T^2 through a semi-empirical theory. The temperature-structure parameter has the form

$$C_T^2 = (79 \times 10^{-6} P/T^2)^{-2} C_N^2 \quad (1)$$

C_T^2 can be estimated by several methods of measurement. Two of these methods will be discussed here.

At a separation distance, r , of the order of inertial subrange scales, the temperature structure function in a locally isotropic field has the form

$$\overline{[T(x) - T(x + r)]^2} = C_T^2 r^{2/3} \quad (2)$$

C_T^2 can be found by making simultaneous measurements of temperature, at two positions separated by the distance r . A second method for determination of C_T^2 is by its relation to the one dimensional temperature spectrum which has the inertial subrange form

$$\phi_T(K) = \beta C_T^2 K^{-5/3} \quad (3)$$

where β is a constant and K is the streamwise component of wave number.

Indirect means of expression C_T^2 in terms of other meteorological parameters is through turbulence similarity theory. Surface-layer-similarity theory predicts that when the statistics of the mean and turbulent flow fields are properly non-dimensionalized, they become universal functions of only a stability parameter. Wyngaard, et al (1971) chose to use the Richardson number, Ri, as the stability parameter in doing calculations from overland data. The Richardson number is defined by

$$Ri = \frac{g/\bar{T}\ (d\theta/dz)}{(d\bar{u}/dz)^2} \tag{4}$$

where g = acceleration of gravity, $\bar{T}$ = mean temperature, $d\theta/dz$ = potential temperature gradient, and $d\bar{u}/dz$ = mean wind speed gradient. It was shown by Wyngaard that the temperature structure function could be expressed as a function of the Richardson number, potential temperature gradient and height.

$$C_T^2 = z^{4/3}\ (d\theta/dz)^2\ f\ (Ri) \tag{5}$$

The results of Wyngaard's calculations are shown in Figure 2, verifying the similarity theory prediction for unobstructed overland data.

In order to fully understand the relation of C_T^2 to turbulence, one must consider ε and ε_θ, the viscous dissipation of turbulent kinetic energy and the viscous dissipation of temperature, through theoretical relations. Both the balance expression for turbulent kinetic energy and Kolmogorov's hypotheses must be examined. These theoretical considerations are reviewed in the following paragraphs.

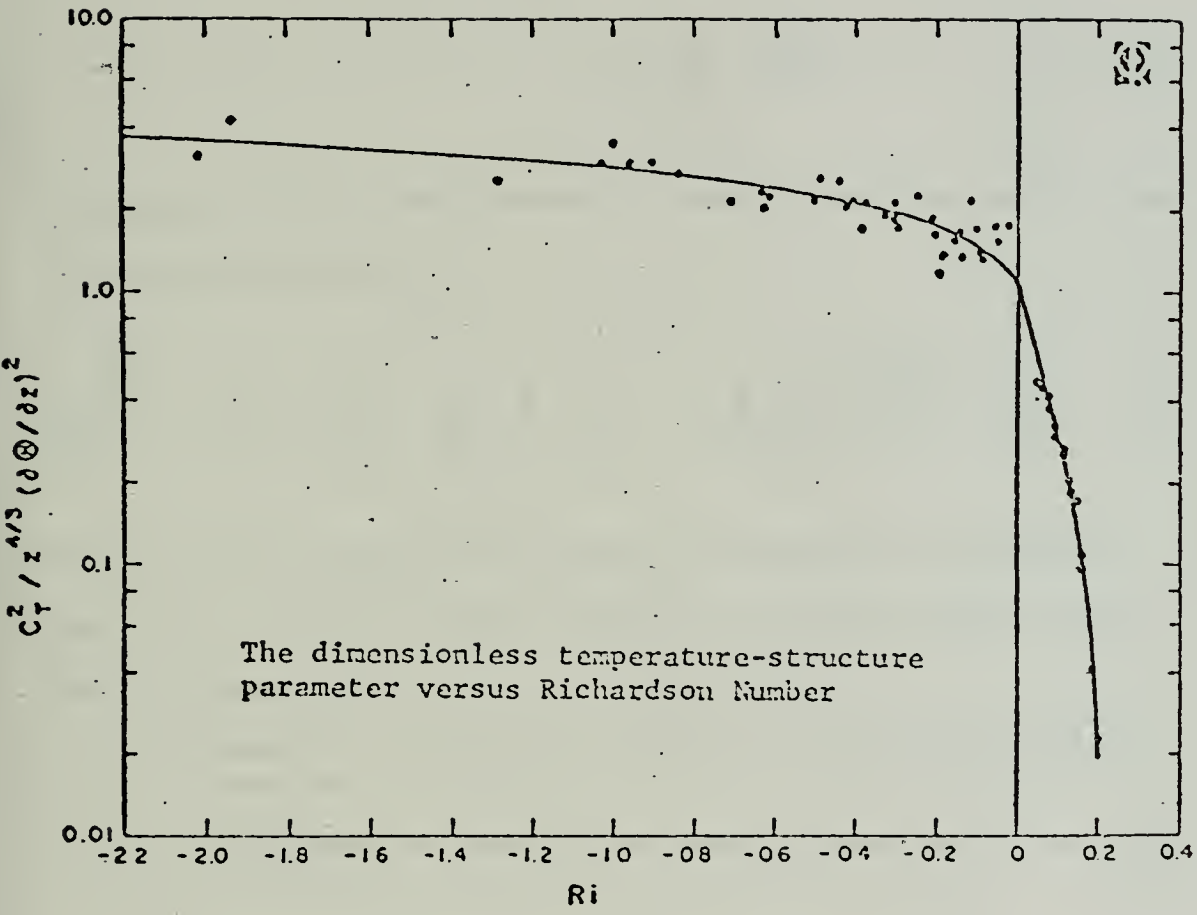
10.0
1.0
0.1
0.01
$C_T^2 / z^{4/3} (\partial\Theta/\partial z)^2$
The dimensionless temperature-structure
parameter versus Richardson Number
-2.2
-2.0
-1.8
-1.6
-1.4
-1.2
-1.0
-0.8
-0.6
-0.4
-0.2
0
0.2
0.4
Ri

Figure 2.

B. BALANCE EXPRESSION FOR TURBULENT KINETIC ENERGY

The turbulent kinetic energy balance expression has the following general form

$$\frac{\partial}{\partial t}\left(\frac{\overline{v_i^2}}{2}\right) = -\overline{v_i v_j}\,\frac{\partial \bar{u}_i}{\partial x_j} + \frac{g}{T_o}\,\overline{v_i\theta}\,\delta_{i_3} - \varepsilon + \frac{\partial}{\partial x_j}\left[\overline{v_j\left(-\frac{P}{\rho} - \frac{v_i v_i}{2}\right)}\right] - \frac{\partial}{\partial x_j}\left[\bar{u}_j\,\overline{\frac{v_i v_i}{2}}\right] \qquad (6)$$

Neglecting horizontal eddy transports, energy flux in the vertical can be expressed as follows

$$\frac{\partial}{\partial t}\left(\frac{\overline{v_i^2}}{2}\right) = -\overline{v_3 v_i}\,\frac{\partial \bar{u}_i}{\partial x_3} + \frac{g}{T_o}\,\overline{v_i\theta}\,\delta_{i_3} - \varepsilon - \frac{\partial}{\partial x_3}\left[\overline{v_3\left[\left(\frac{v_i v_i}{2}\right) + \frac{P}{\rho}\right]}\right] \qquad (7)$$

The four terms on the right hand side of the equation represent processes which will cause a time variation of turbulent kinetic energy. These processes are

i) Mechanical production of turbulent kinetic energy from the mean flow

ii) Archimedes work term or the energy released due to the effects of buoyancy

iii) Viscous dissipation of turbulent kinetic energy

iv) Pressure work and flux divergence of turbulent kinetic energy due to transfer by turbulent motion

Further simplification of the kinetic energy balance expression can be made by making several definitions and assumptions:

i) Assuming that the turbulent kinetic energy is in a statistically steady state,

$$\frac{\partial}{\partial t}\left(\frac{\overline{v_i^2}}{2}\right) = 0$$

ii) Assuming horizontal homogeneity (i.e., the spatial variations of mean fluctuations are negligible),

$$\frac{\partial}{\partial x} = \frac{\partial}{\partial y} = 0$$

iii) Specifying the co-ordinate system such that

$$\bar{u}_2 = \bar{u}_3 = 0$$

iv) Assuming the divergence terms are negligible

$$\frac{\partial}{\partial x_3} \overline{[v_3 (\frac{v_i v_i}{2}) + \frac{P}{\rho}]} = 0$$

The turbulent kinetic energy balance expression can then be expressed in the following simplified form, for the case when the mechanical production of turbulent kinetic is equal to the viscous dissipation plus energy released or gained due to buoyance effects

$$-\overline{v_1 v_3} \frac{\partial \bar{u}_1}{\partial x_3} = \varepsilon - \frac{g}{T_o} \overline{v_3 \theta} \qquad (8)$$

In cases where the atmosphere is in near-neutral stability conditions, the second term on the right hand side of the equation is negligible and Equation (8) can be written as

$$u_*^2 \frac{\partial \bar{u}}{\partial x_3} = \varepsilon \qquad (9)$$

where $u_*^2 = -\overline{v_1 v_3}$. The following expression for the vertical gradient of the mean wind also applies to the neutral condition

$$\frac{\partial \bar{u}_1}{\partial x_3} = \frac{u_*}{Kz} \qquad (10)$$

where K is a universal non-dimensional constant (i.e., the Von Karman constant) and Z is height. Combining Equations (9) and (10) yields an expression to estimate u_* based on measurements of ε at a known height Z

$$\varepsilon = \frac{u_*^3}{KZ} \tag{11}$$

C. VARIATION OF ε WITH HEIGHT

Equation (11) can be used to verify the constant flux assumption. A straight line plot, with a -1 slope, of $\ln\varepsilon$ against $\ln Z$ implies u_* is a constant with height. For non-neutral stratification in the atmosphere, one must retain the buoyancy term in Equation (8). Equation (11) can be modified as follows to include the buoyancy effects.

$$\varepsilon = \frac{u_*^3}{KZ}\left[\phi_1\left(\frac{Z}{L}\right) - \frac{Z}{L}\right] \tag{12}$$

or

$$\varepsilon = \frac{u_*^3}{KZ}\left[\phi_2\,(Ri)\right] \tag{13}$$

where $L = -\bar{T}u_*^3/gK\,\overline{v_3\theta}$ (Monin-Obuhkov Length)

$\overline{v_3\theta}$ = heat flux

Ri = Richardson number

ϕ_1 = empirical function of Z/L

ϕ_2 = empirical function of Ri

Equation (13) can be written in the following form

$$\ln\varepsilon = -\ln Z + \ln\phi_2(Ri) + \ln\left(\frac{u_*^3}{K}\right) \tag{14}$$

From overland experiments, various expressions for ϕ_1 and ϕ_2 have been derived. For cases of neutral stability, very little variation from a -1 slope is noted in a plot of $\ln \varepsilon$ versus $\ln Z$. In cases of instability, an effect on the plot of $\ln \varepsilon$ versus $\ln Z$ is to increase the slope (in a negative sense), to greater than -1. Figure 3 illustrates these effects.

D. VARIATION OF C_T^2 WITH HEIGHT

Equation (5) expressed C_T^2 as a function of the Richardson number, potential temperature gradient and height. The potential temperature gradient can be expressed in the following manner

$$\frac{d\theta}{dZ} = -\frac{T_*}{Z} \; g_1 \left(\frac{Z}{L}\right) \tag{15}$$

where $T_* = \overline{v_3\theta}/Ku_*$

L = Monin-Obuhkov Length

g_1 = empirical function of stability

The Richardson number can also be expressed as a function of Z/L in Equation (5)

$$Ri = g_2 \left(\frac{Z}{L}\right) \tag{16}$$

Combining Equation (5) and Equation (16) results in the following expression for C_T^2

$$C_T^2 = T_*^2 \, Z^{-2/3} \, g_3 \left(\frac{Z}{L}\right) \tag{17}$$

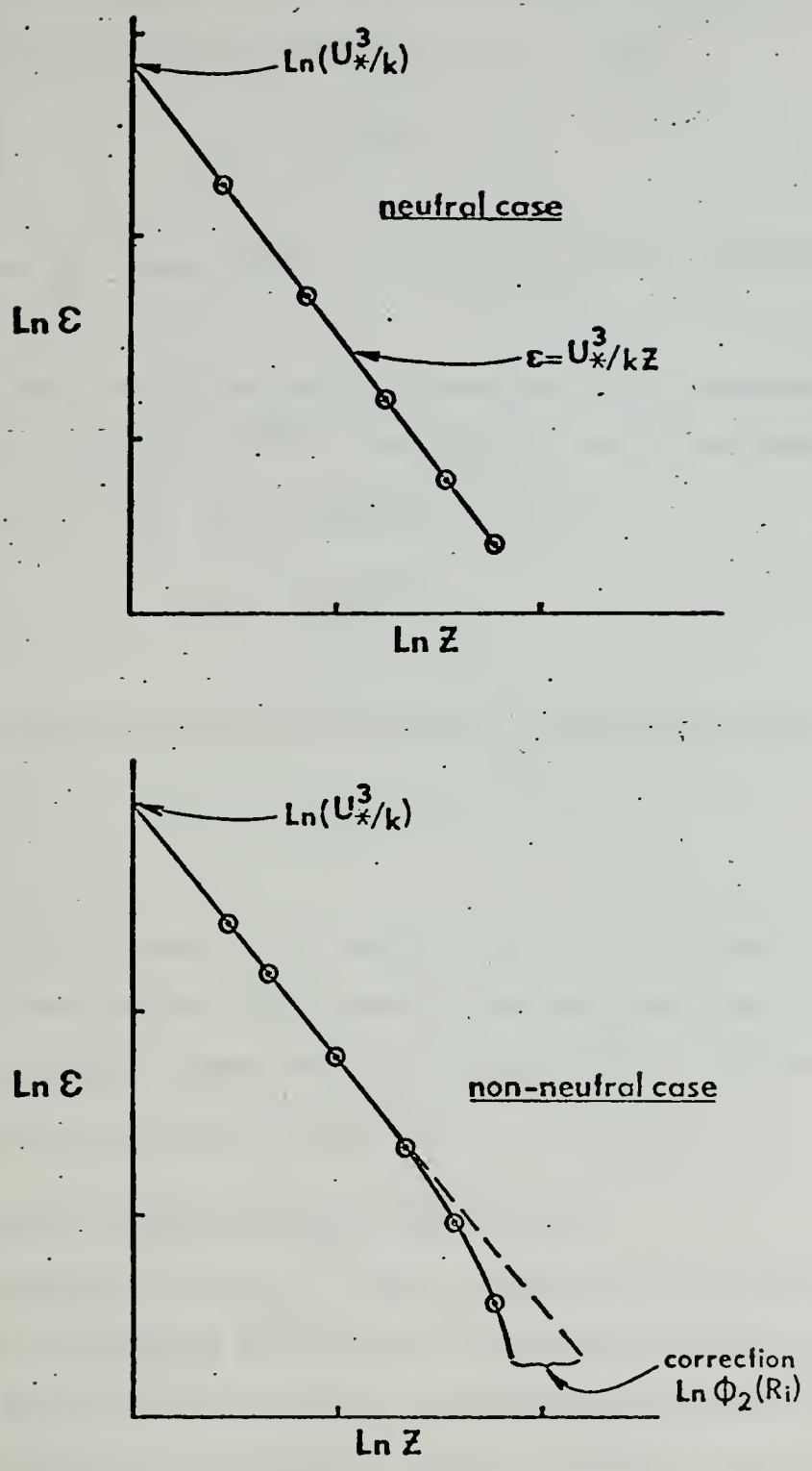

Figure 3. An Illustration of the Effect of Stability on the Variation of ε with Height

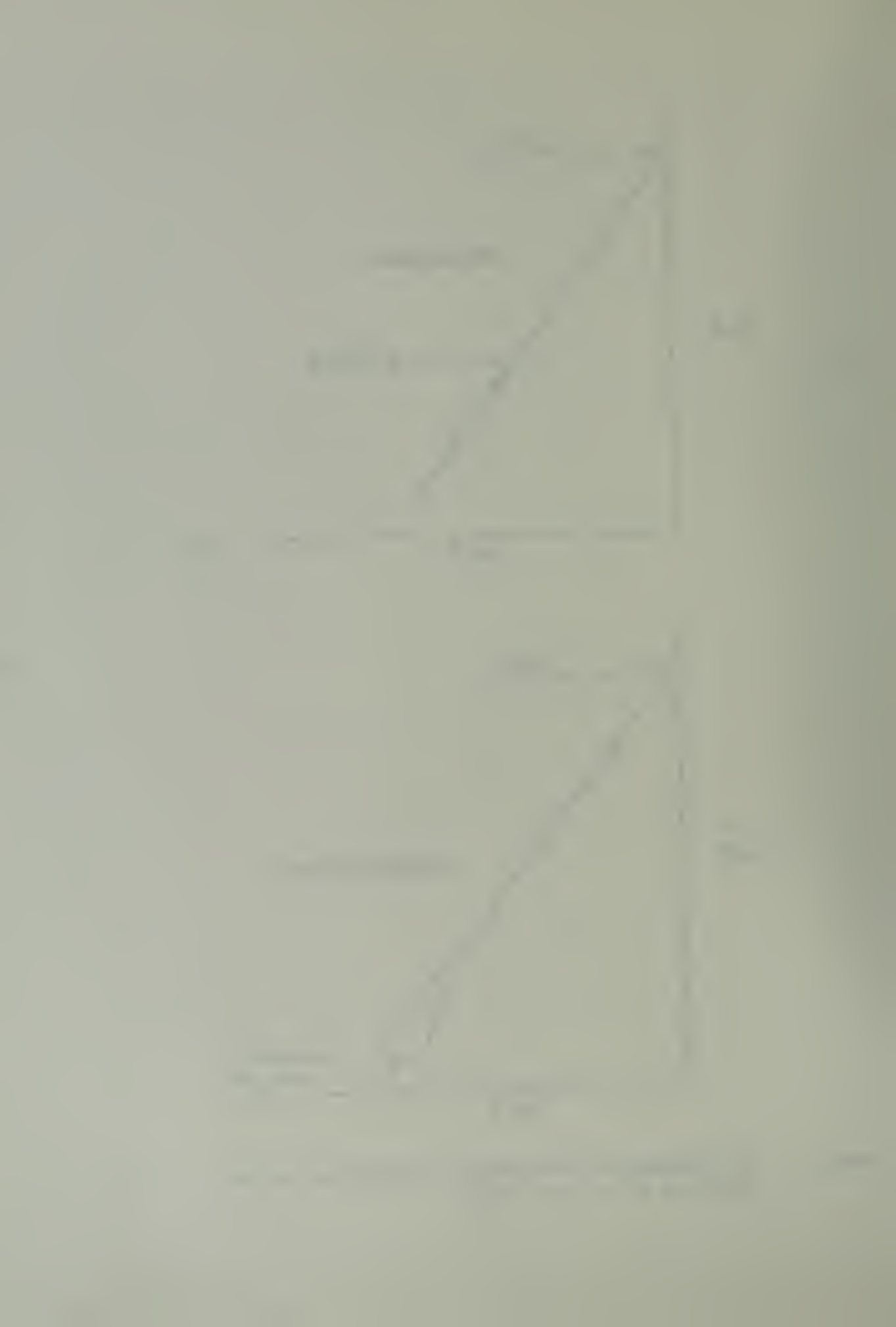

where g_3 is an empirical function of stability derived from overland data. For cases of neutral stability, $g_3 = 1$, and

$$C_T^2 = T_*^2 \, Z^{-2/3} \tag{18}$$

A plot of ln C_T^2 versus ln Z would yield a straight line with a -2/3 slope.

Under stable conditions Wyngaard noted that C_T^2 decreased with height more slowly than $Z^{-2/3}$. For unstable conditions, overland results indicate that g_3 approximates the function

$$g_3 \simeq \frac{4}{3} \left(\frac{Z}{L}\right)^{-2/3} \tag{19}$$

Also, for unstable conditions, Equation (17) can be expressed as

$$C_T^2 \simeq \frac{4}{3} T_*^2 \, (-L)^{2/3} \, Z^{-4/3} \tag{20}$$

A plot of ln C_T^2 versus ln Z would yield a straight line plot with a slope of approximately -4/3, assuming overland results are valid over water. Figure 4 shows the predicted variation of C_T^2 with height for various stability conditions.

E. KOLMOGOROV'S SPECTRAL SIMILARITY EXPRESSIONS

The parameters ε and C_T^2 can be estimated on the basis of Kolmogorov's expressions for universal spectra (in the inertial subrange) of both fluctuating velocity and temperature spectra. The inertial subrange in the velocity spectrum represents a range of eddy

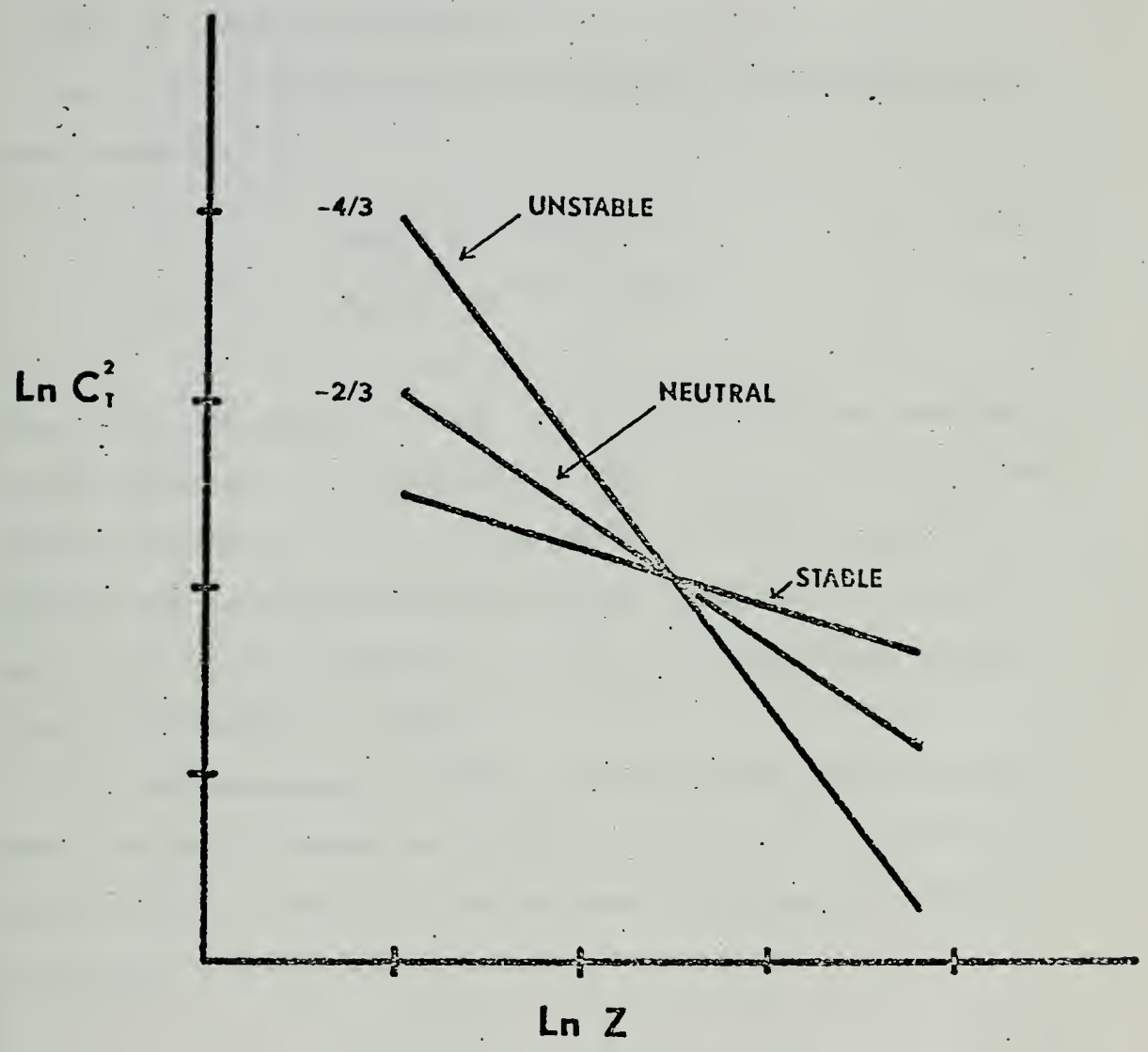

Figure 4. An Illustration of the Effect of Stability on the Variation of C_T^2 with Height

sizes where energy is transferred from the production region to the dissipation region, (i.e., from lower to higher wave numbers). Figure 5 from Lumley and Panofsky (1964) shows the separate regions of a typical turbulence spectrum.

According to Kolmogorov's second hypothesis, the following functional relations hold

$$\phi(K) = C_1 \varepsilon^{2/3} K^{-5/3} \tag{21}$$

$$\phi_T(K) = C_2 \varepsilon^{-1/3} \varepsilon_\theta K^{-5/3} \tag{22}$$

where $\phi(K)$ and $\phi_T(K)$ represent one dimensional velocity and temperature spectra and K represents the wave number. C_1 and C_2 are empirical constants. C_T^2 is defined to be $\varepsilon^{-1/3}\varepsilon_\theta$; therefore, Equation (22) is identical to Equation (3). Equations (21) and (22) can be used to find estimates of ε and C_T^2 by examining respective velocity and temperature spectra.

Turbulent measurements are made at a fixed point in the flow and hence spectra are obtained for temporal frequency f . In order to use Equations (21) and (22), time and space scales must be related using Taylor's (1938) "frozen turbulence" hypothesis

$$K = 2\pi f/\bar{u} \tag{23}$$

where $\bar{u}$ is the mean wind speed. The hypothesis implies that turbulence remains unchanged during the time required for it to sweep past the probe. The following forms of Equations (21) and (22) feature

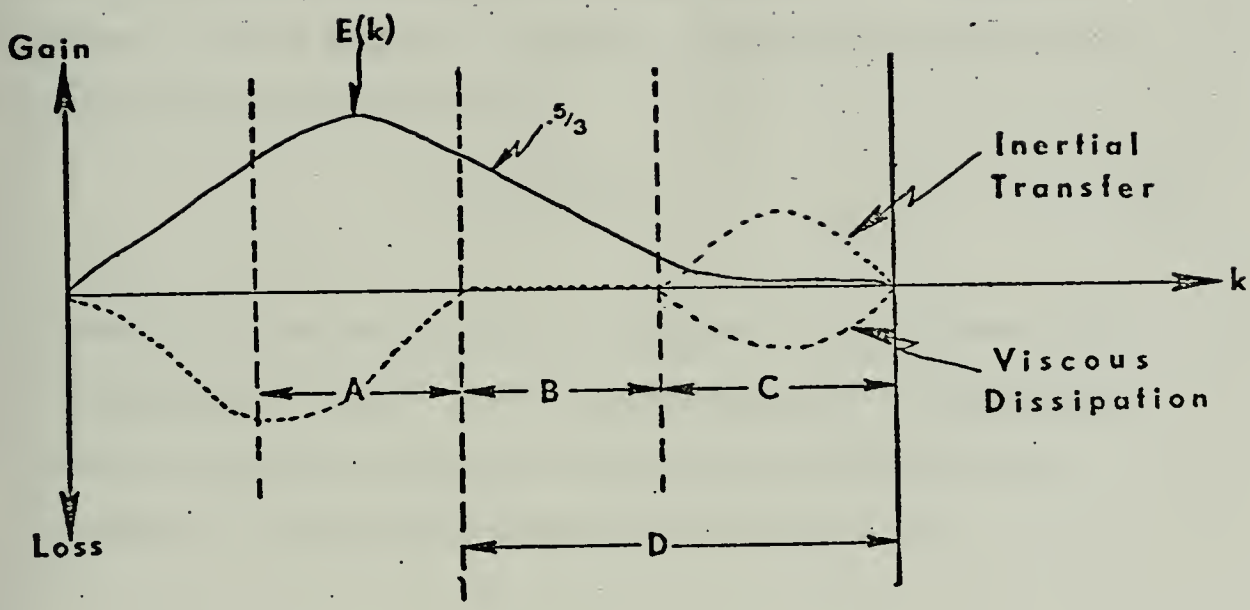

Figure 5. A Schematic Drawing Showing Spectral Transfer and Illustrating (A) Energy Containing Region (B) Inertial Subrange (C) Dissipation Range and (D) Universal Equilibrium Range

the transformation from frequency to wave number

$$f\,\phi(f) = K\,\phi(K) = C_1\,\varepsilon^{2/3}\,K^{-2/3} \tag{24}$$

$$f\,\phi_T(f) = K\,\phi_T(K) = C_2\,C_T^{\,2}\,K^{-2/3} \tag{25}$$

A second method for estimating ε results from examining the upper limit of the inertial subrange of a velocity spectrum. In statistical equilibrium, a spectrum of turbulence is independent of the source of the turbulence and depends only on ε, γ and K where γ is the kinematic viscosity. The following expression is applicable for the inner scale

$$lo = (\gamma^3/\varepsilon)^{1/4} \tag{26}$$

where $(lo)^{-1}$ is proportional to the dissipation wave number. The dissipation wave number can be obtained from spectra which show scale separation between the inertial subrange and viscous dissipation regions. ε can then be determined from Equation (26).

III. OBSERVATIONS

A. DATA COLLECTION

Observational experiments were made from the R/V ACANIA anchored in Monterey Bay approximately two miles offshore. Observations were made at three levels on the forward mast and bow of the ACANIA. Figure 6 shows the mounting arrangements during the experiments.

B. EQUIPMENT

1. Fluctuating Velocity and Temperature Measurements

Velocity sensors were (TSI) Model 1210 "hot wire" probes with sliding support shields. Calibration of the sensors was made prior to the experiments. Band filtering was applied to the signal with cut-off frequencies of 2 hz and 2 khz respectively. The signals were then amplified and recorded on a 14 channel Sangamo Model 3562 FM recorder.

Temperature sensors used were (TSI) Model 1210 platinum wire probes with sliding support shields. Electronic conditioning similar to that applied to the velocity signals was applied to the temperature signals. The temperature data was analog recorded simultaneously with the velocity data.

2. Mean Velocity, Temperature and Humidity Measurements

Mean velocity measurements were made at each level using C. W. Thornthwaite cup anemometers. The cup revolutions were counted by Hewlett Packard 5221A electronic counters. Direct readout of mean wind data were then made and recorded in a log. Mean temperature measurements at each level were made using Hewlett Packard quartz thermometers.

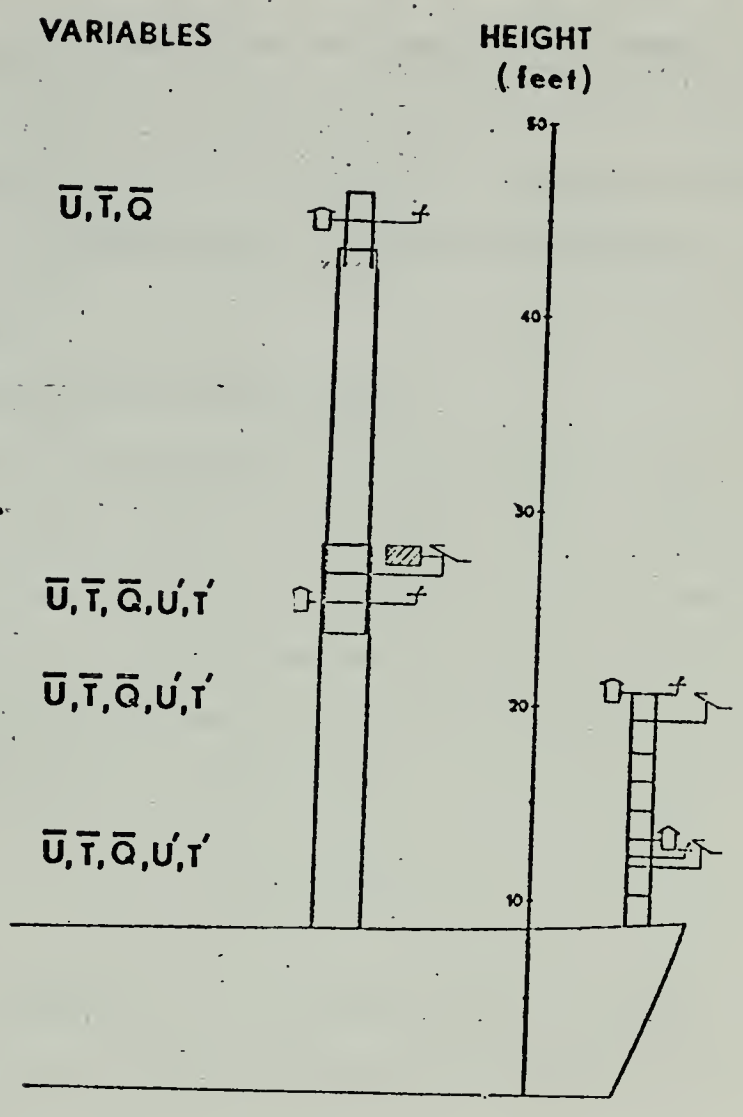

Figure 6. Mounting Arrangements

The signals were passed to a printer, allowing the temperature data to be printed out in a time series. Humidity data were collected in a fashion analogous to temperature data using a Hydrodynamics Digital II system and a printer.

Figures 7 and 8 show the electronics involved in processing both mean and fluctuating data in the ACANIA's laboratory.

C. CALIBRATION

1. Calibration of Hot Wire Sensors

Velocity fluctuation measurements were made with hot wire sensors. These velocity sensors were calibrated before each experiment using a manometer and TSI 1125 Calibrator in accordance with procedures outlined by Johnston (1974). For any given mean wind speed, there is a corresponding voltage output. The relationship between wind speed and voltage is described by the following equation

$$v^2 = a(u)^{1/2} + b \tag{27}$$

where v is voltage and u is the wind speed. Constants a and b are calibration curve slope and intercept respectively, and are determined experimentally.

To analyze the recorded velocity data it was necessary to determine a calibration factor such that

$$c \times v' = u' \tag{28}$$

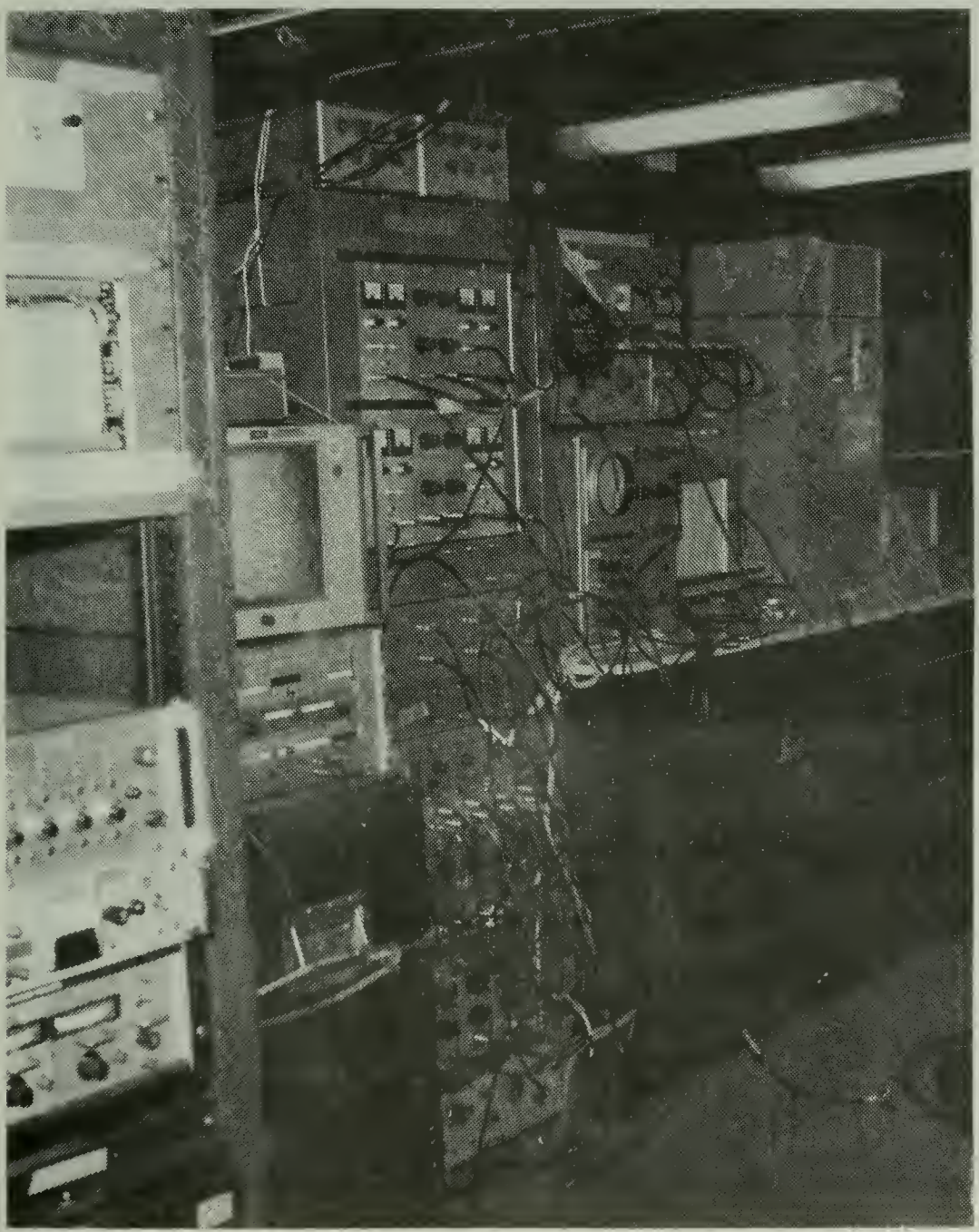

Figure 7. Equipment Used Aboard R/V ACANIA to Obtain Fluctuating Velocity and Temperature Data.

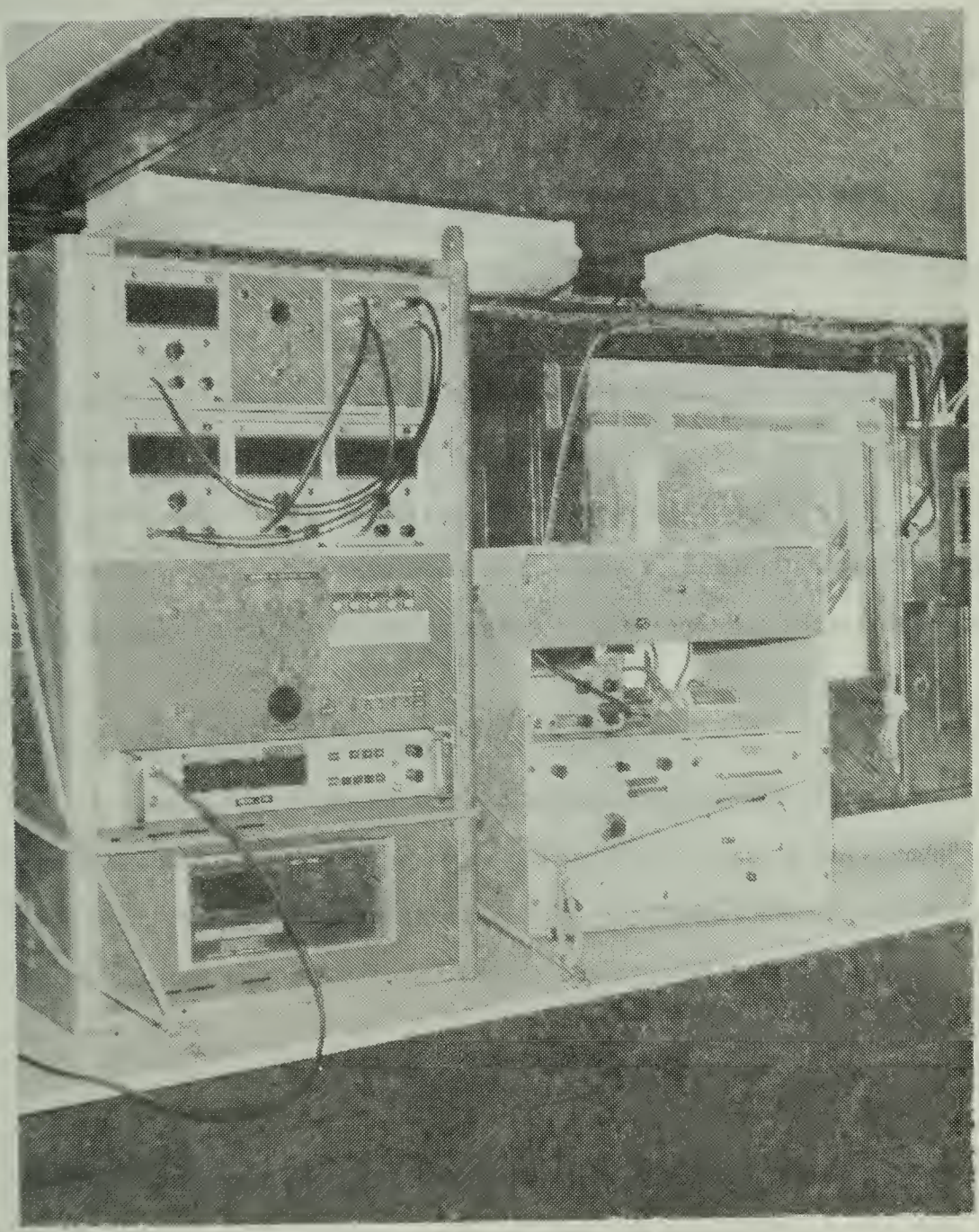

Figure 8. Equipment Used Aboard R/V ACANIA to Obtain Mean Velocity and Temperature Data.

where c = calibration factor, v' = voltage fluctuation and u' = velocity fluctuation. Differentiation of Equation (27) yields

$$\left[\frac{4vu}{a}^{1/2}\right] v' = u' \tag{29}$$

where c , the calibration is then determined by the relation

$$c = \left[\frac{4vu}{a}^{1/2}\right] \tag{30}$$

For analysis, determination of the calibration factor consisted of (1) obtaining the slope of the calibration curve (2) selecting a mean wind speed value observed during the experiment and (3) entering the calibration curve with this mean wind value to determine a corresponding voltage. Figure 9 is an example of an actual hot wire calibration curve.

2. Calibration of Platinum Wire Sensors

Temperature fluctuation measurements were made using platinum wire sensors. A small temperature fluctuation causes a corresponding resistance change in the platinum wire. The resistance of a given wire can be related to temperature through the following equation

$$R = Ro\ (1 + \alpha\ (T-To)) \tag{31}$$

where R = resistance, T = temperature, To = 0°C, Ro = resistance at 0°C, and α = a constant for platinum. The resistance, in ohms, can be measured at any given temperature and thus Ro determined for each

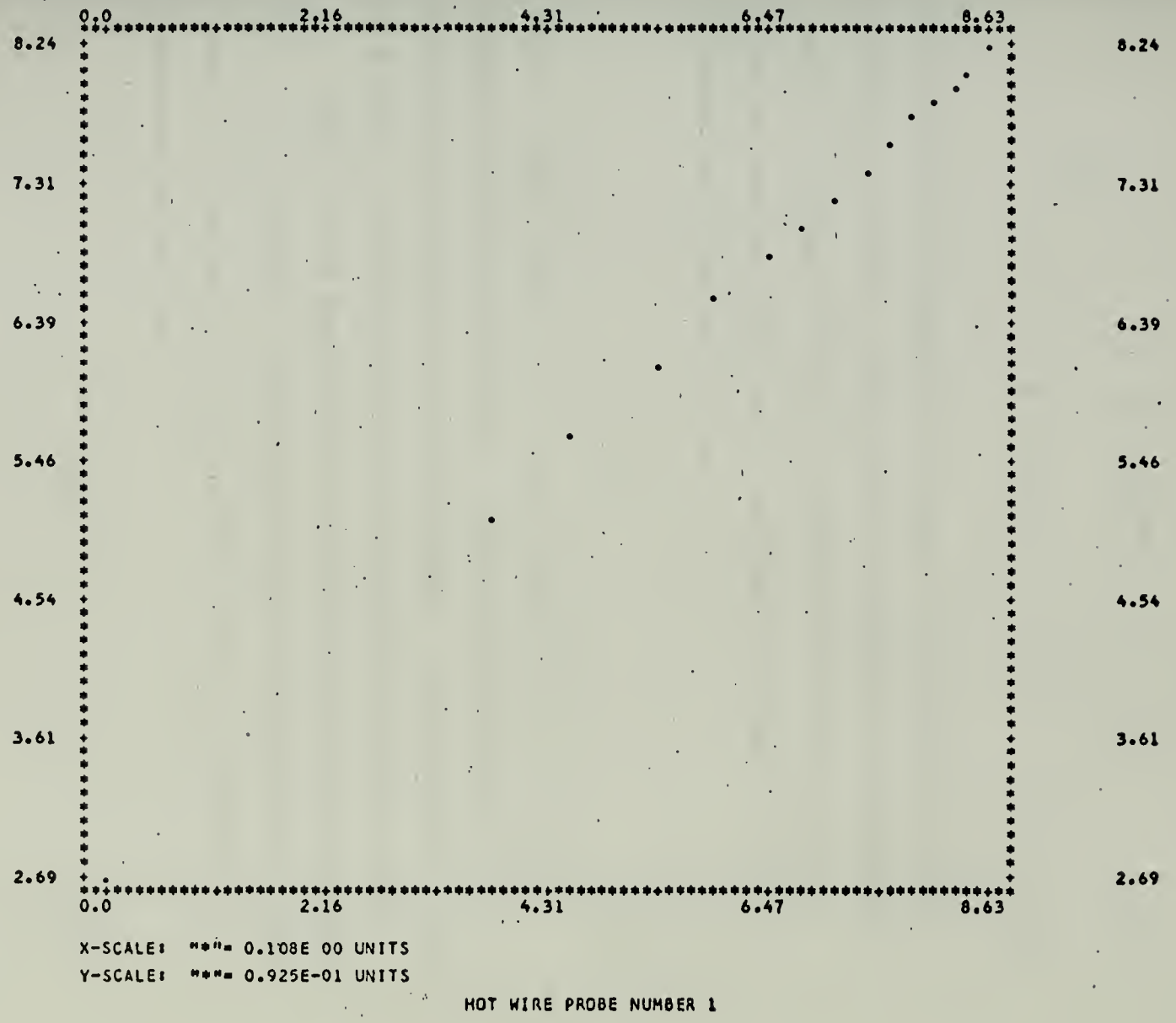

Figure 9. Hot Wire Calibration Plot

wire. Differentiating Equation (31) results in

$$dR = \alpha \, Ro \, dT \tag{32}$$

or

$$R' = \alpha \, Ro \, T' \tag{33}$$

which relates a small temperature change to a small change in the resistance of the wire. During analysis, resistance fluctuations are recorded as voltage fluctuations, through the electronics involved. A transfer function, which relates resistance to voltage, must be determined during calibration, i.e.,

$$v' = HR' \tag{34}$$

H , the transfer function can be found by substituting a variable resistor in place of the wire and recording voltage changes as a function of corresponding resistance changes. By plotting these points on a graph, the resultant slope will determine the transfer function H . Figure 10 is an example of an actual calibration curve used during one of the experiments. Substituting Equation (34) into Equation (33) results in an expression to relate recorded voltage fluctuations to temperature fluctuations

$$T' = \left(\frac{1}{H\alpha Ro}\right) v' \tag{35}$$

or

$$T' = C_H v' \tag{36}$$

where C_H is the calibration factor.

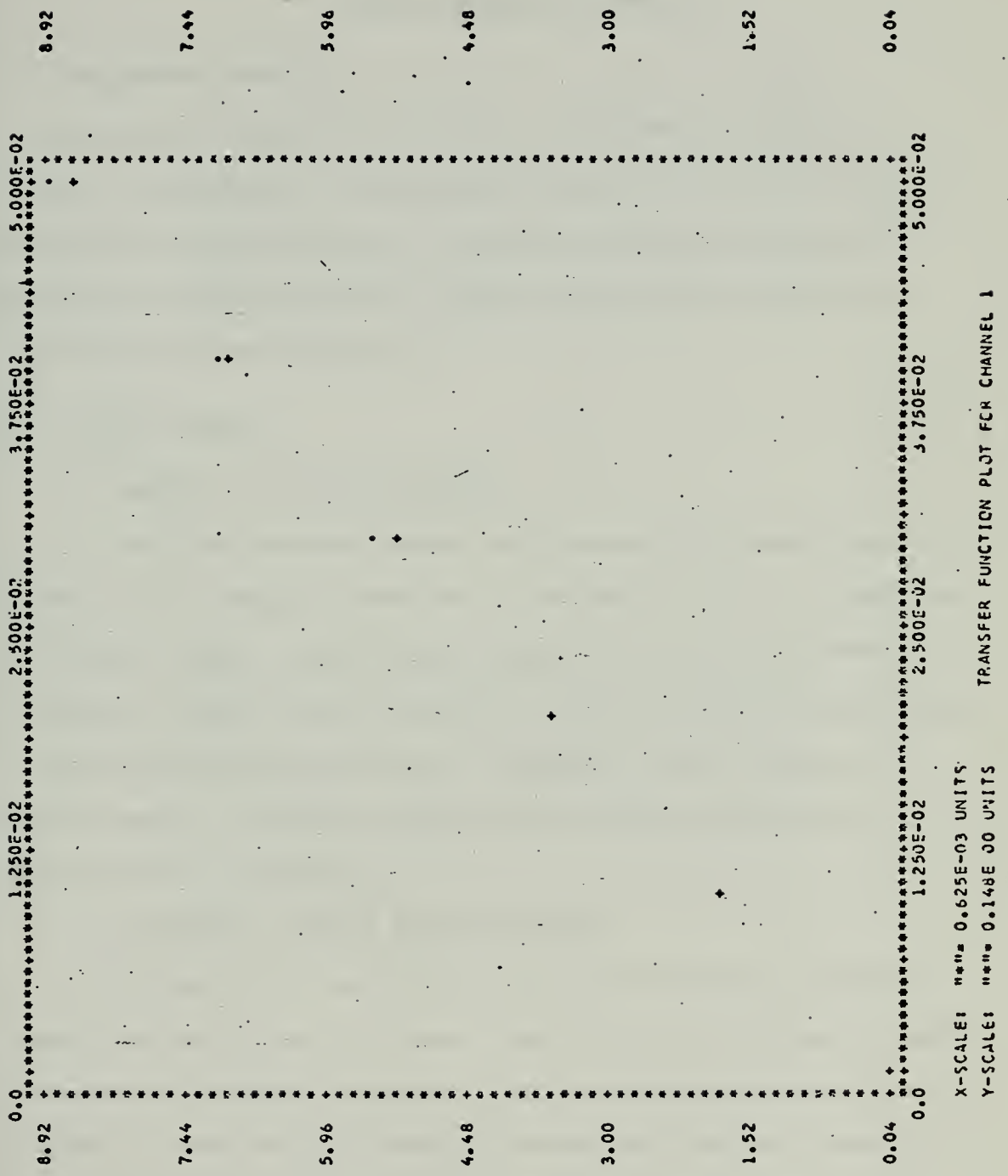

Figure 10. Platinum Wire Transfer Function Plot

IV. DATA REDUCTION AND ANALYSIS

A. PRELIMINARY ANALYSIS

Data period selection was based on evaluations of strip chart records of the signals. Criteria for selection of data periods consisted of (1) signal strength (2) possible averaging time and (3) availability of mean profiles. Typical signals meeting the above criteria are shown in Figure 11.

B. DIGITAL METHODS

1. Analog to Digital Conversion

Data from selected periods were prepared for further analysis by an analog to digital conversion of the magnetic tapes as described by Johnston (1974). The analog to digital process was performed on the hybrid computer system located on the fifth floor of Spanagel Hall at the Naval Postgraduate School. The hybrid system consists of an analog computer, COMCOR Ci 5000, interfaced electrically with a digital computer, XDS 9300.

2. Seven Track to Nine Track Conversion

The analog to digital process yields seven-track octal based records written on a digital tape. Analysis of the data was then performed on an IBM-360/67 computer. This computer requires nine-track hexadecimal based digital records. Conversions from seven-track to nine-track tapes were made with procedures described in Naval Postgraduate School Computer Center Technical Note #0211-08. Two programs used for this conversion were TAPEOUT and CONVERT.

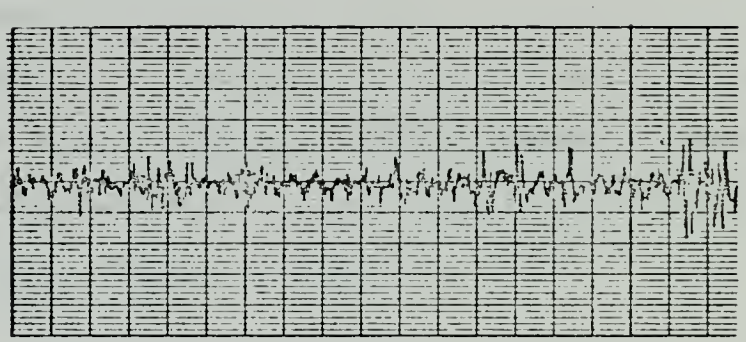

Typical Velocity Signal

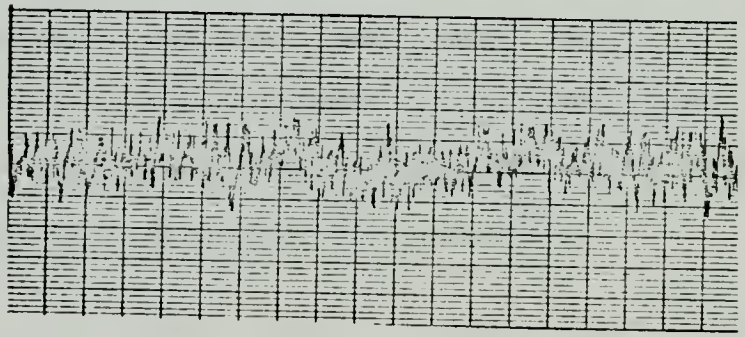

Typical Temperature Signal

Figure 11

3. Digital Analysis Programs

Spectral analysis of the digital tapes was made using FTOR (Fast Fourier Transform) and SCOR (Spectral Analysis), programs which are available in the IBM 360/67 library. Descriptions of the FFT program package have been described by McKendrick (1972) and Johnston (1974). The output of th4 SCOR program consists of a tabular computer printout as shown in Figure 12 and a graphical plot of the spectrum versus frequency as shown in Figure 13.

C. SCALING PROCEDURES

During observational and analysis procedures, several gains and scaling factors were applied to the recorded signals. Prior to recording the data, an amplitude gain was applied to the signals. During the analog to digital process an additional gain was applied to the signal along with a scaling factor. The scaling factor resulted from the consideration that the maximum voltage input to the COMCOR Ci 5000 is 100 volts, and this corresponds to a digital maximum of 2^{23} on the XDS 9300. Applying the respective gain and scaling factors resulted in a signal input to the IBM 360/67 as follows

$$v(\text{volts}) \times G1 \times G2 \times SC = v(\text{volts IBM 360}) \qquad (37)$$

where v = signal from velocity or temperature unit

G1 = amplification prior to recording

G2 = amplification during A-D process

SC = analog to digital scaling factor

The spectral analysis programs yielded plots of the energy density function $\phi(f)$, versus frequency f. The corresponding units

SPECTRUM STATISTICS FOR 2941 CHANNEL 5 T' LEVEL 1
STATISTICS ARE BASED ON 528 BLOCKS OF 1024 SAMPLES EACH
THE SAMPLING FREQUENCY WAS 512.0000 SAMP/SEC , MAKING THE BLOCK LENGTH 2.00000 SECONDS
TREND IS THE AVERAGE OF (VALUE(A)-VALUE(B))/(BLOCK NO.(A)-BLOCK NO.(B))
A CALIBRATION FACTOR OF 1.000E 00 HAS BEEN APPLIED TO THE INPUT DATA

	FREQUENCY HERTZ	BANDWIDTH	SPECTRUM (VOLTS)**2/HERTZ	STD.DEV.	TREND	FREQ*SPECTRUM (VOLTS)**2	LAST HARMONIC
1	4.33E-01	5.00E-01	5.13E 11	6.14E 11	3.020E 08	2.220E 11	1
2	9.68E-01	5.00E-01	1.75E 11	1.92E 11	4.407E 07	1.699E 11	2
3	1.48E 00	5.00E-01	9.78E 10	1.10E 11	-1.278E 07	1.446E 11	3
4	1.98E 00	5.00E-01	6.52E 10	7.29E 10	1.768E 07	1.294E 11	4
5	2.70E 00	1.00E 00	3.80E 10	3.54E 10	1.805E 07	1.027E 11	6
6	3.72E 00	1.00E 00	2.47E 10	2.45E 10	1.473E 07	9.197E 10	8
7	4.94E 00	1.50E 00	1.46E 10	1.26E 10	4.651E 06	7.204E 10	11
8	6.68E 00	2.00E 00	9.16E 09	7.81E 09	2.890E 05	6.116E 10	15
9	8.91E 00	2.50E 00	6.06E 09	5.00E 09	2.376E 06	5.397E 10	20
10	1.19E 01	3.50E 00	3.84E 09	3.34E 09	1.441E 06	4.557E 10	27
11	1.58E 01	4.50E 00	2.47E 09	2.16E 09	9.586E 05	3.918E 10	36
12	2.10E 01	6.00E 00	1.81E 09	2.23E 09	1.631E 05	3.813E 10	48
13	2.80E 01	8.00E 00	1.32E 09	1.53E 09	1.811E 05	3.696E 10	64
14	3.73E 01	1.10E 01	6.91E 08	6.04E 08	2.902E 05	2.580E 10	86
15	5.00E 01	1.45E 01	4.18E 08	3.39E 08	1.230E 05	2.090E 10	115
16	6.66E 01	1.90E 01	2.65E 08	2.06E 08	5.790E 04	1.767E 10	153
17	8.86E 01	2.55E 01	2.10E 08	1.45E 08	3.069E 04	1.856E 10	204
18	1.18E 02	3.45E 01	9.40E 07	6.63E 07	1.104E 04	1.112E 10	273
19	1.58E 02	4.55E 01	8.07E 07	4.17E 07	-1.815E 03	1.274E 10	364
20	2.11E 02	6.10E 01	3.60E 07	1.96E 07	-4.254E 03	7.576E 09	486
21	2.50E 02	1.30E 01	3.22E 07	1.61E 07	-1.257E 04	8.045E 09	512

INTEGRAL (SUM) UNDER SPECTRUM = 6.23E 11 VOLTS **2
ZEROTH HARMONIC (DC) HAD
AVERAGE = 5.08E 05 VOLTS
VARIANCE = 1.03E 12 VOLTS **2
TREND = 7.59E 02 VOLTS

Figure 12. SCOR Spectral Statistics

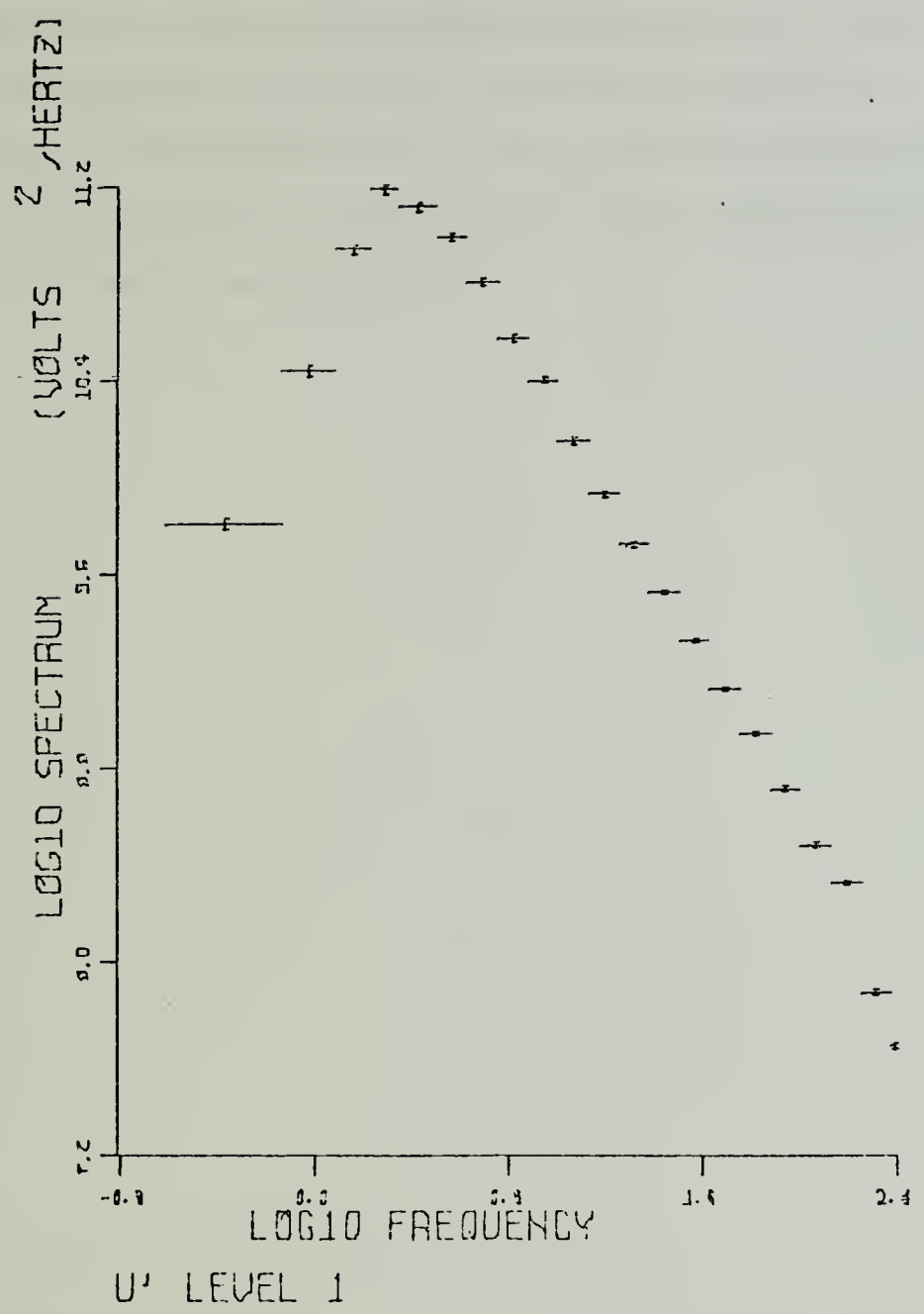

Figure 13. SCOR Spectral Plot

associated with $\phi(f)$ and f were $VOLT^2SEC$ and $1/SEC$ respectively. Multiplying each point of the energy density function by its corresponding frequency $\phi(f)f$ results in a quantity with the units of $VOLTS^2$. Taking the square root of this quantity, one can relate VOLTS to VOLTS' (IBM 360) through Equation (37). Final scaling was accomplished by using Equations (29) and (35) which relates volts to either velocity or temperature fluctuations respectively.

V. INTERPRETATION OF SPECTRA

A. SINGLE POINT METHOD

The Single Point Method is perhaps the most straightforward method used to obtain ε and C_T^2 from velocity and temperature spectra. From the spectrum, a wave number, K, within the inertial subrange is chosen. Using Equations (21) and (22), calculations of ε and C_T^2 can then be made directly.

B. INTERCEPT METHOD

A second method described by Johnston (1974) can also be used to evaluate ε and C_T^2 from velocity and temperature spectra. This method has an advantage over the single point method in that many points are used to evaluate the spectral estimate. This is accomplished by taking the average slope through many points and determining an intercept value as discussed in the following paragraphs.

1. Determination of ε

Equation (24) can be written in the following form

$$\ln K\phi(K) = -2/3 \ln K + \ln C_1\varepsilon^{2/3} \tag{38}$$

Plotting $\ln K\phi(K)$ against $-2/3 \ln K$ results in a curve with a slope of +1 and an intercept of $\ln C_1\varepsilon^{2/3}$. At the point of intercept, $\ln K$ equals zero and

$$\ln K\phi(K) = \ln C_1\varepsilon^{2/3} \tag{39}$$

Letting A equal $\ln K\phi(K)$, the intercept value, ε then becomes

$$\varepsilon = \left(\frac{e^A}{C_1}\right)^{3/2} \tag{40}$$

By determining the intercept value, ε can be estimated. Figure 14 shows a typical plot of this type using velocity data at three levels.

2. Determination of C_T^2

A similar procedure can be used to determine C_T^2. Equation (25) can be written as follows

$$\ln K\phi_T(K) = -2/3 \ln K + \ln C_2 C_T^2 \tag{41}$$

Using the same procedure as described in the determination of ε, C_T^2 can be evaluated at the point of intercept in the following manner

$$C_T^2 = \frac{e^B}{C_2} \tag{42}$$

where $B = \ln K\phi_T(K)$ at the ordinate intercept. Figure 15 is an example of an intercept plot using temperature data at two levels.

C. INNER SCALE METHOD

A third method of estimating ε was to consider the inner scale. Equation (26) describes an expression relating ε to the separation between the inertial subrange and dissipation region of the spectra. By choosing the wave number at which the dissipation region occurs in the velocity spectra, ε can be evaluated. This method was quite subjective with regard to determining the exact point of scale separation. However, the results were qualitatively good when compared to the intercept method.

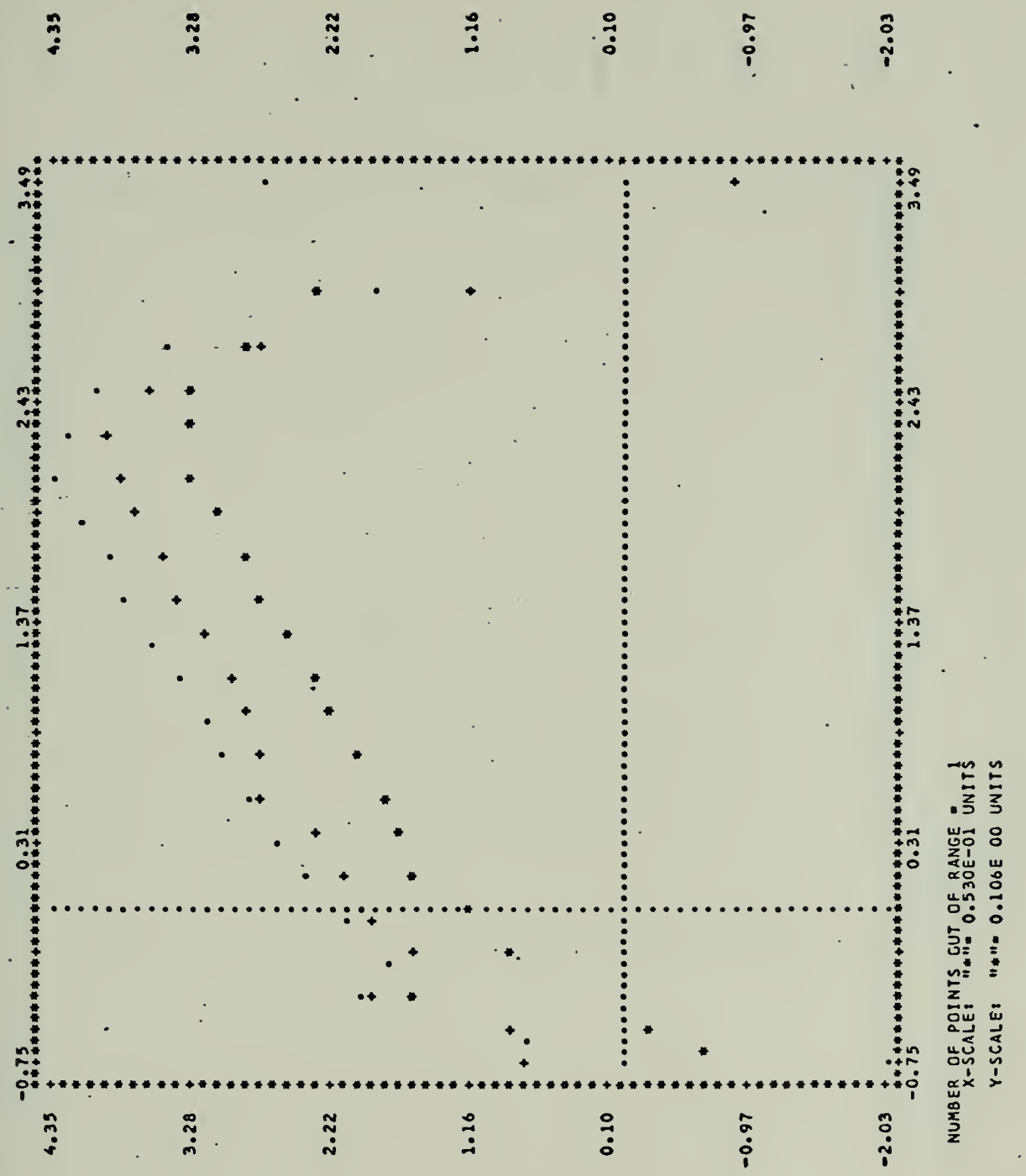

Figure 14. Intercept Plot for Velocity Data at Three Levels.

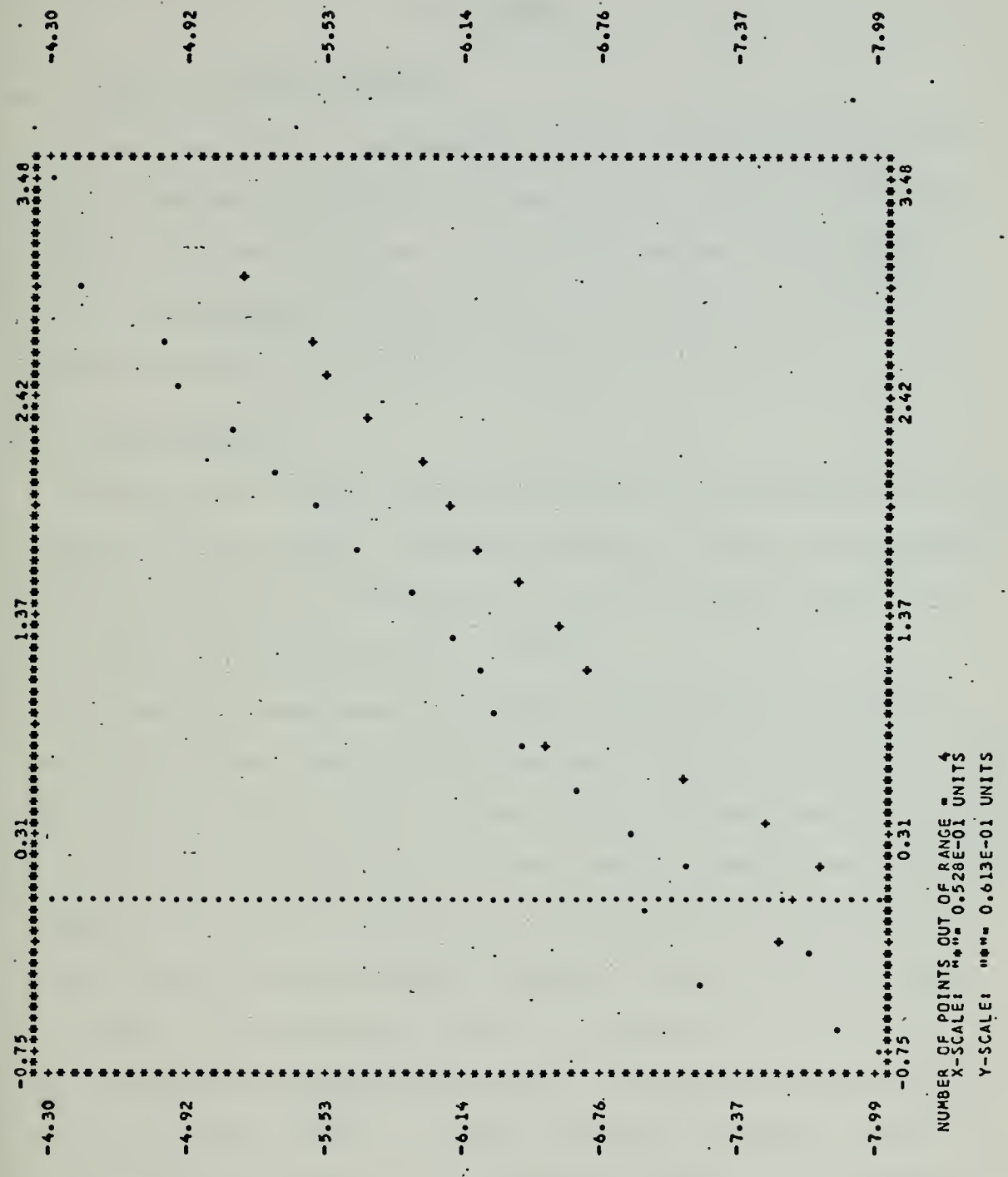

Figure 15. Intercept Plot for Temperature Data at Two Levels.

VI. RESULTS

A. SUMMARY OF PERIODS EXAMINED

Fluctuating velocity and temperature data were collected from three levels aboard the R/V ACANIA on 18 January 1974. Selected periods for analysis were chosen for three time intervals between 1834 and 1932. Table I lists periods examined, heights at which data were collected, parameters measured and stability conditions for each period.

B. VELOCITY RESULTS

Velocity spectra were obtained for simultaneous measurements at three levels during each period. From these spectra ε and u_* were computed by methods described in Sections V-B-1 and V-C. Table II lists ε and u_* calculations for each of these periods.

The original experimental plans were to measure mean wind data at each of the levels. Due to problems encountered with the read-out counter, the wind data appeared to be in error. The problem was resolved by use of mean wind measurements at one level, the ACANIA's aerovane, and then estimating a vertical wind field based on the Monin-Obuhkov prediction. A Fortran computer program, PROPAR, described by Cardone (1969) was used to estimate the vertical wind field. This program uses inputs of (1) mean wind speed (2) anemometer height (3) air-sea temperature difference and (4) thermometer height to compute the output parameters. These computed parameters included (1) u_* = friction velocity (2) Zo = roughness parameter and (3) L = Monin-Obuhkov Length. Mean wind was calculated at each level using the following equation

TABLE I

Data Periods Considered in This Study

18 January 1974

Time (local)	Height (cm)	Parameter	Stability (Ri)
1834-1854	394.0 (level 1)	$\bar{U},\bar{T},\bar{Q},U',T'$	-0.136
	658.0 (level 2)	$\bar{U},\bar{T},\bar{Q},U',\Delta T'$	
	822.0 (level 3)	$\bar{U},\bar{T},\bar{Q},U',T'$	
1855-1913	394.0 (level 1)	$\bar{U},\bar{T},\bar{Q},U',T'$	-0.293
	658.0 (level 2)	$\bar{U},\bar{T},\bar{Q},U',\Delta T'$	
	822.0 (level 3)	$\bar{U},\bar{T},\bar{Q},U',T'$	
1914-1932	394.0 (level 1)	$\bar{U},\bar{T},\bar{Q},U',T'$	-0.923
	658.0 (level 2)	$\bar{U},\bar{T},\bar{Q},U',\Delta T'$	
	822.0 (level 3)	$\bar{U},\bar{T},\bar{Q},U',T'$	

TABLE II

ε and Momentum Flux Calculations for 18 January 1974 using the Zero Intercept Method

Height	ε ($cm^2\ sec^{-3}$)	u_* ($cm\ sec^{-1}$)
	Time 1834-1854	
394.0	83.43	23.60
658.0	54.74	24.33
822.0	22.83	19.57
	Time 1855-1913	
394.0	342.96	37.80
658.0	79.21	27.51
822.0	36.72	22.93
	Time 1914-1932	
394.0	112.28	26.05
658.0	13.67	15.32
822.0	22.22	19.40

$$u = \frac{u_*}{K} \left(\ln \left(\frac{Z}{Zo} \right) - \psi_1 \left(\frac{Z}{L} \right) \right) \qquad (43)$$

where ψ_1 is an empirical function of Z/L described by Paulson (1970). The purpose in defining the wind field distribution was to obtain advection speeds for relating temporal and spatial frequencies. The need for wave number (spatial frequency) description was identified in Section II-E.

Figures 16, 17 and 18 show typical velocity spectra at each level for one of the periods. In each case a -5/3 slope is observed for the inertial subrange region. At higher frequencies, the spectra exhibit greater slopes. The regions of different slopes represent different scales in the turbulent regime. The scale represented by greater slope at higher frequencies, is the dissipation region. Closer investigation reveals a decrease in the frequency where the slope changes as height increases. However, as mentioned earlier and as can be seen here, the exact point of scale separation between the inertial subrange and dissipation region is difficult to determine.

Results on ε versus height for the velocity data are shown in Figures 19, 20 and 21 where $\ln \varepsilon$ is plotted against $\ln Z$ for each data period. Negative slopes, greater than -1, are noted in each case. As stated in Section II-C, this agrees with present boundary layer theory for unstable atmospheric conditions.

The deviation of the slope from -1 was examined to see if it could be accounted for by the influence of the unstable stratification. The plots were corrected for stability using Equation (13) where $\phi_2 = (1 - 12Ri)^{-1/4}$. A slight shift toward a -1 slope was observed; however,

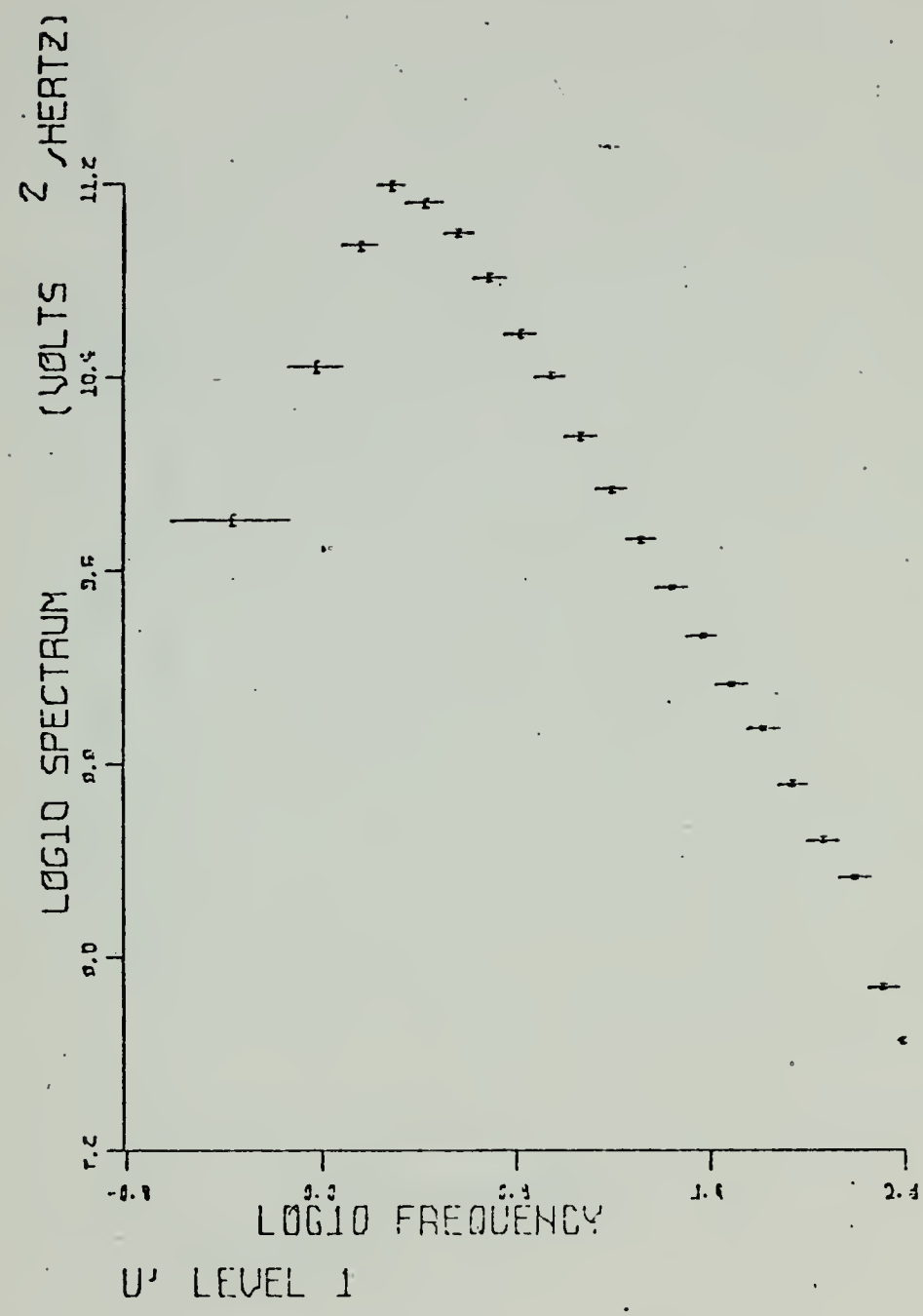

Figure 16. Velocity Spectrum Level 1 for 1855-1913, 18 Jan 74.

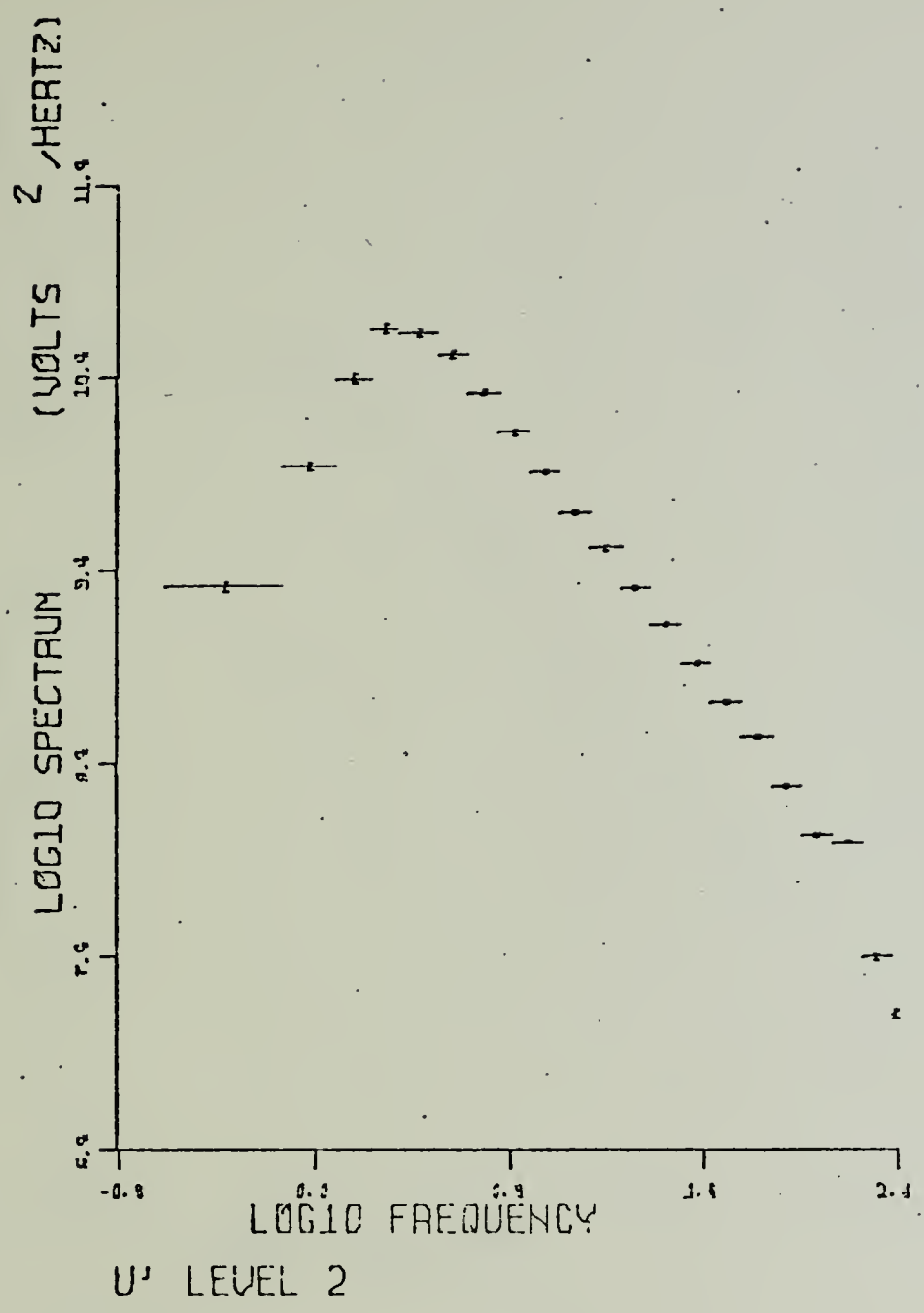

Figure 17. Velocity Spectrum Level 2 for 1855-1913, 18 Jan 74.

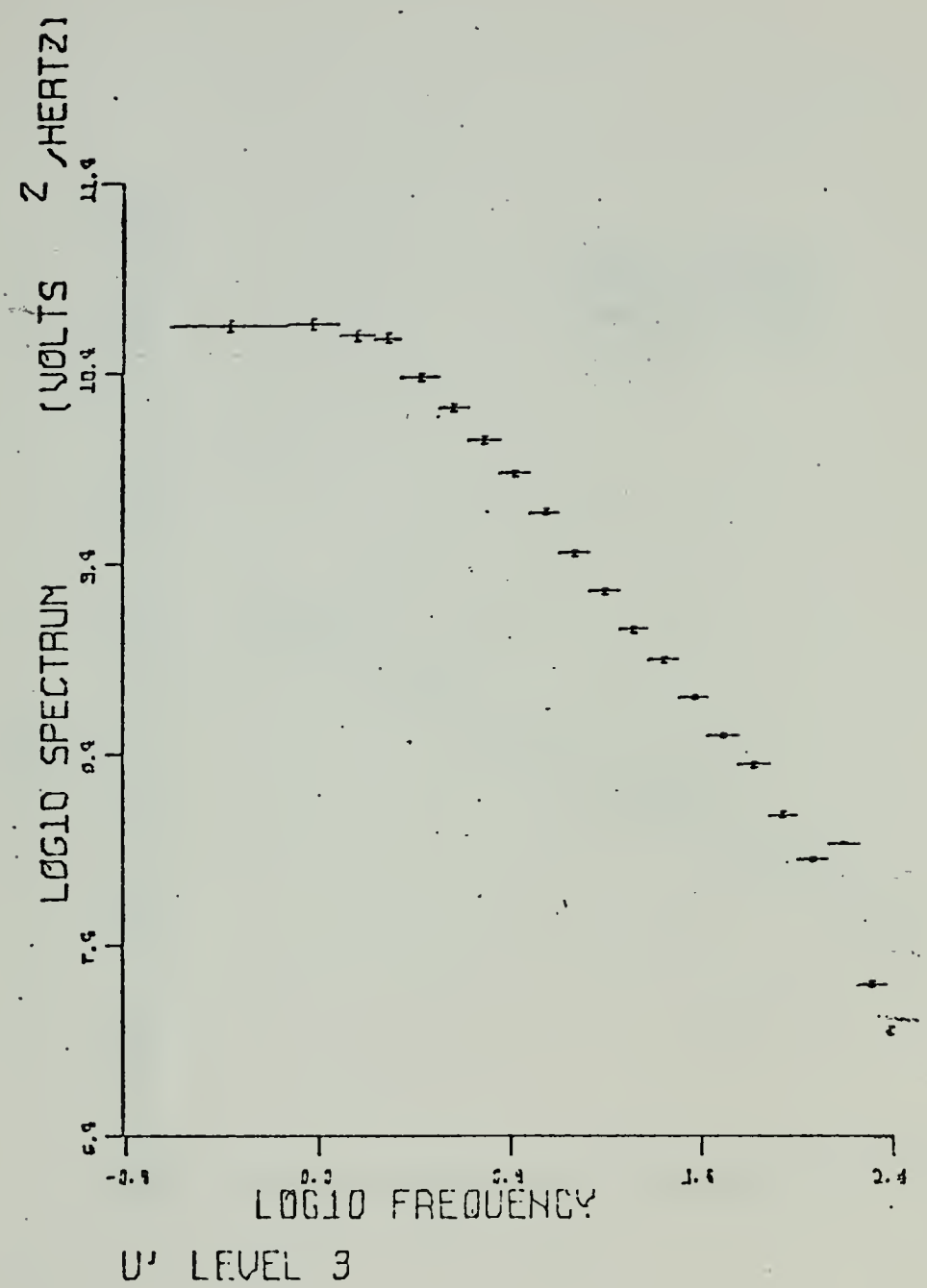

Figure 18. Velocity Spectrum Level 3 for 1855-1913, 18 Jan 74.

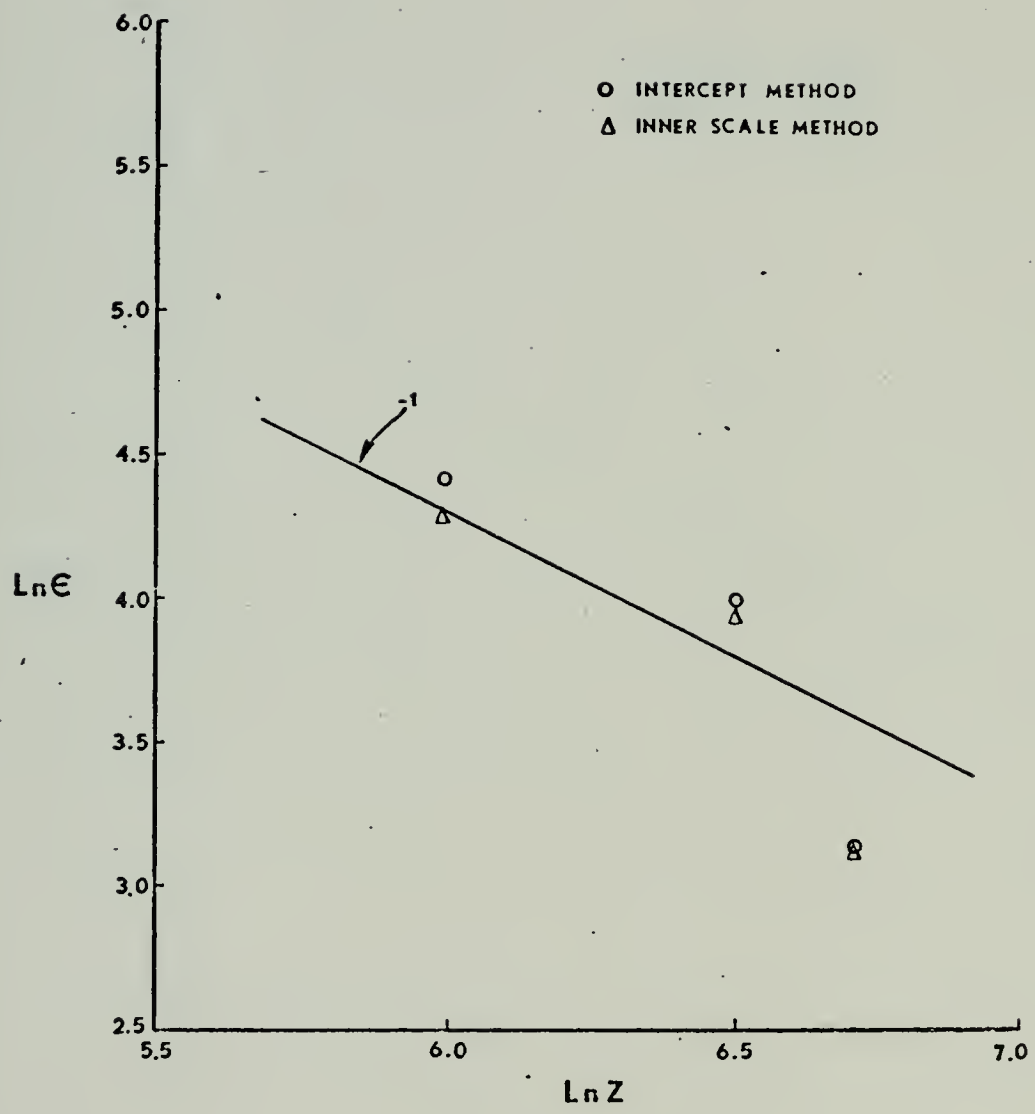

Figure 19. Measured Values of ε vs Height for 1834-1854, 18 Jan 74.

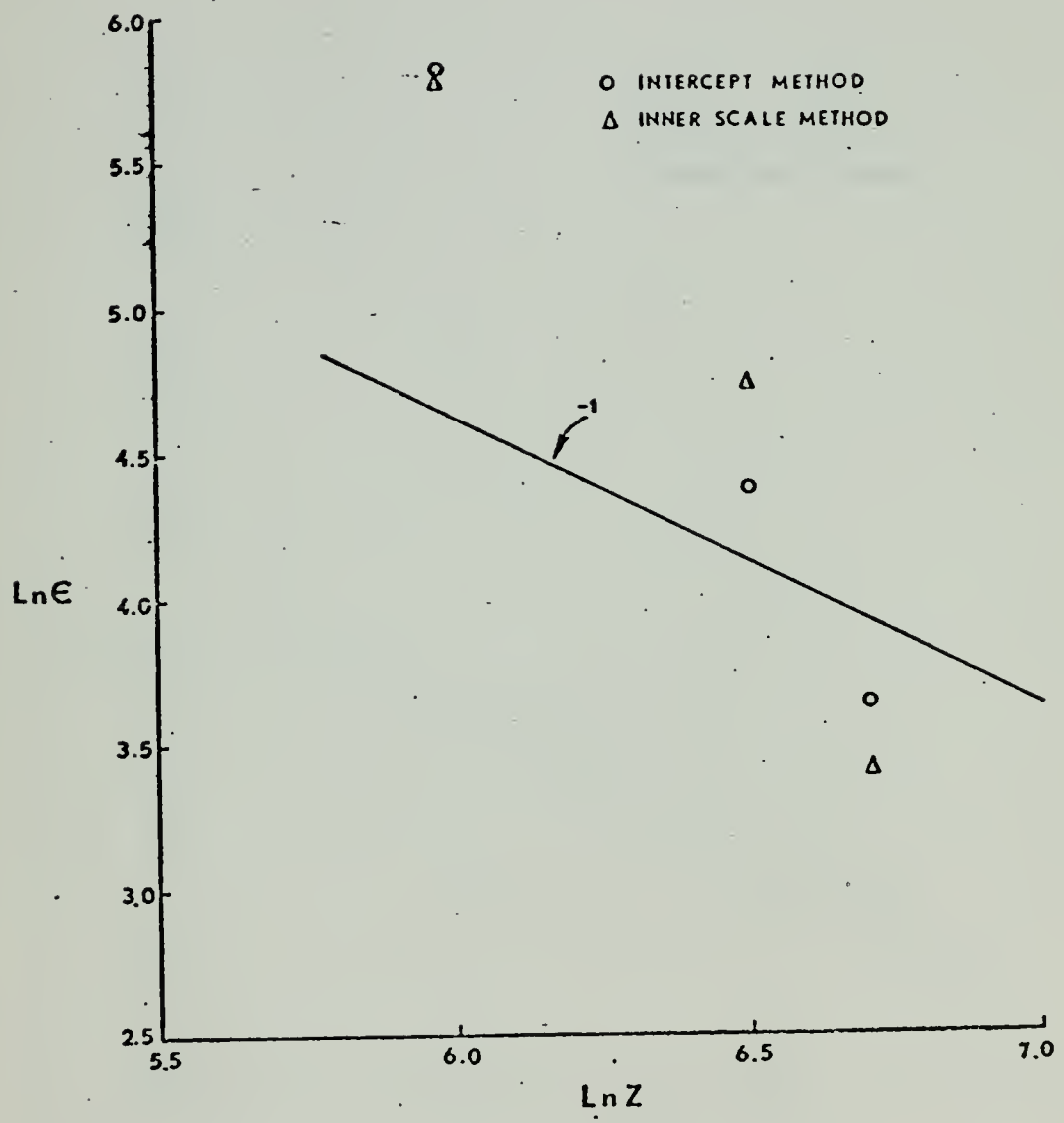

Figure 20. Measured Values of ε vs. Height for 1855-1913, 18 Jan 74.

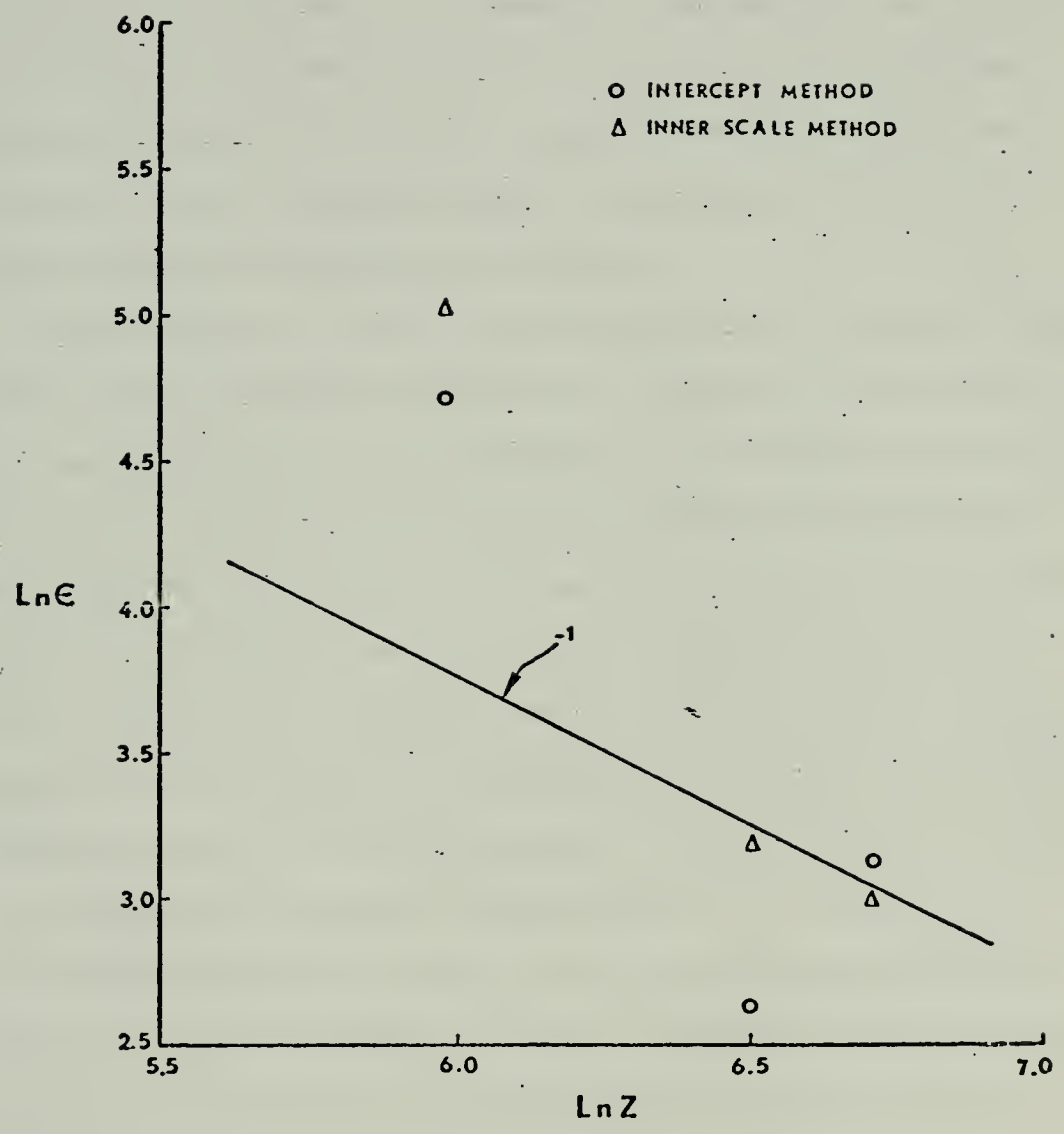

Figure 21. Measured Values of ε vs. Height for 1914-1932, 18 Jan 74.

complete adjustment to a -1 slope was not evident. Similar results were found by Johnston (1974). He states "The fact that the stability corrections did not completely restore the -1 slope, even in the stable case, leads to the examination of the possible effects of wind-wave coupling."

The above results imply that overland prediction for the influence of stability are not completely valid over water and that wind-wave coupling or wave related velocity fluctuations might be the reason. There is still not enough experimental and theoretical knowledge to describe the waves' influence upon the data.

Several consistent features can be observed in the results. During the first two periods there appears to be a bending or "kink" in the plots such that they are concave downward. In the third data period, the "kink" is concave upward. However, strip chart records show a deterioration of the velocity signal at level 2 toward the end of the period. This apparently resulted in low estimates of ε for that level. It is not felt that this "kink" is due to the ship's influence. Welsh (1974) found that ship related motion had little effect on turbulence measurements at these frequencies. Johnston (1974) did not find this characteristic bending in similar plots of $\ln \varepsilon$ versus $\ln Z$ for unstable conditions. In these results, both the intercept method and inner scale method exhibit the "kink". Based on only two periods of analysis, conclusions as to the cause of this feature cannot be asserted.

C. TEMPERATURE RESULTS

Fluctuating temperature data were also obtained at three levels for each period. At levels 1 and 3, C_T^2 was determined from the

one-dimensional temperature spectrum as described by Equations (3) and (22). At the mid level, two probes were separated by $r = 10$ cm and C_T^2 determined by using Equation (2). Table III lists the C_T^2 calculations for each of the periods. Temperature spectra at three levels are shown for one of the periods in Figures 22, 23 and 24. These are typical of the spectra for the other periods examined.

Results of C_T^2 versus height are shown in Figures 25, 26 and 27, where $\ln C_T^2$ is plotted against $\ln Z$. The general slopes of these plots agree reasonably well with the -4/3 prediction for unstable conditions discussed in Section II-D. Periods 1 and 2 both show close agreement with the -4/3 prediction. However, period 3 shows a much greater deviation from -4/3. Comparing Richardson numbers from Table I, it is noted that period 3 was much more unstable than the first two periods. One might expect slightly greater negative slopes for greater instability; however, -4/3 should be a limiting slope if overland results are valid over water. Since C_T^2 is a function of both ε and ε_θ, the possible wind wave effects on ε discussed in the previous section, would also influence C_T^2. This is a possible explanation for any deviation in C_T^2 from a -4/3 slope.

Closer examination of $\ln C_T^2$ versus $\ln Z$ reveals "kinking" or bending similar to that discussed in the velocity results section. In both periods 1 and 2, this bending phenomenon is concave downward as it was for ε calculations. During period 3 the general appearance of the kink in the C_T^2 plot approximates the appearance of the kink in the ε plot, disregarding any influence of a deterioration in the velocity signal during that period. In this case however, the bending is in the opposite direction.

TABLE III

C_T^2 Calculations for 18 Jan 74 using the Zero Intercept Method

Height (cm)	C_T^2 ($°C^2\ cm^{-2/3}$)
	Time 1834-1854
394.0	.00312
658.0	.00239
822.0	.00168
	Time 1855-1913
394.0	.00600
658.0	.00558
822.0	.00428
	Time 1914-1932
394.0	.00934
658.0	.00416
822.0	.00393

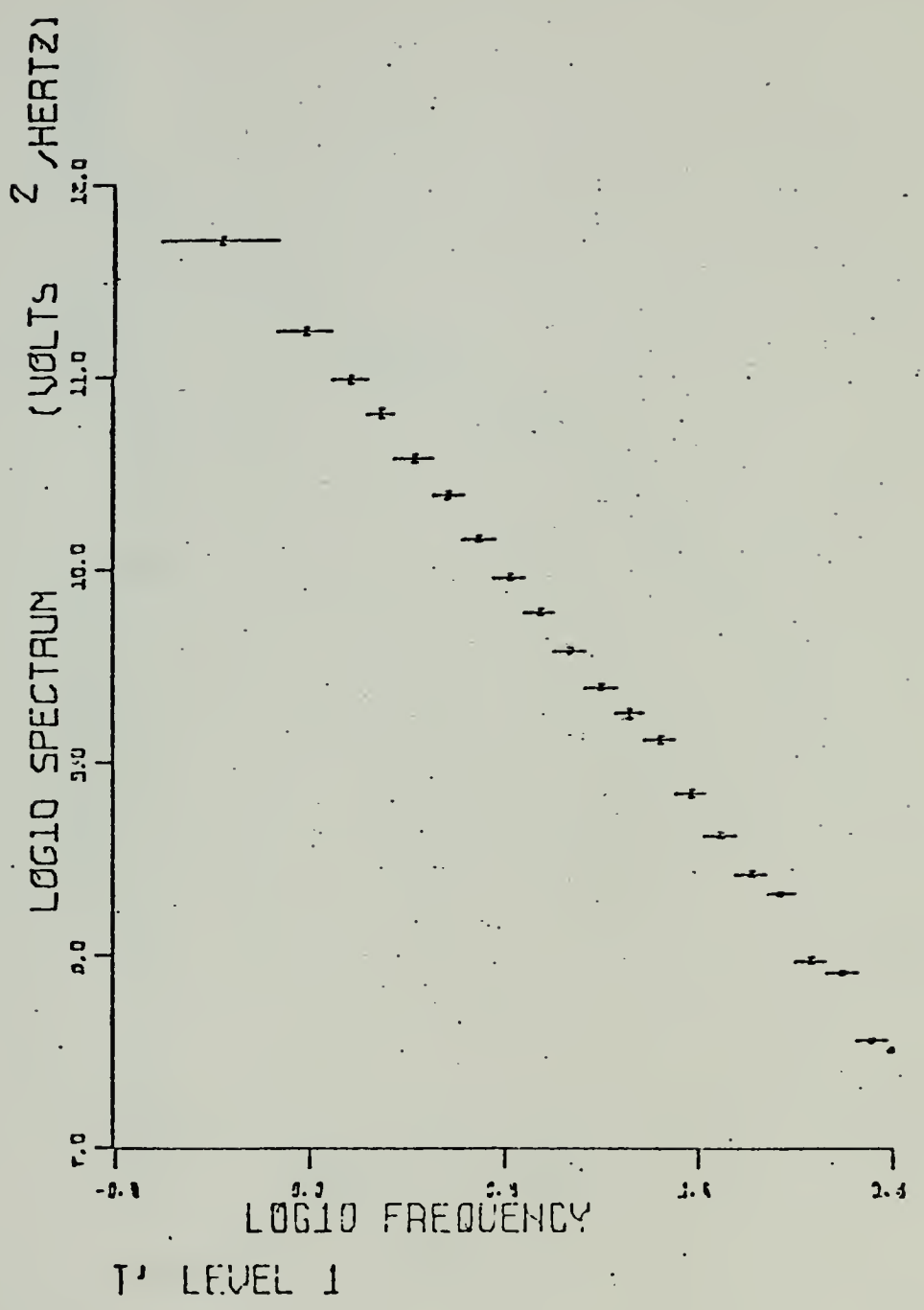

Figure 22. Temperature Spectrum Level 1 for 1855-1913, 18 Jan 74.

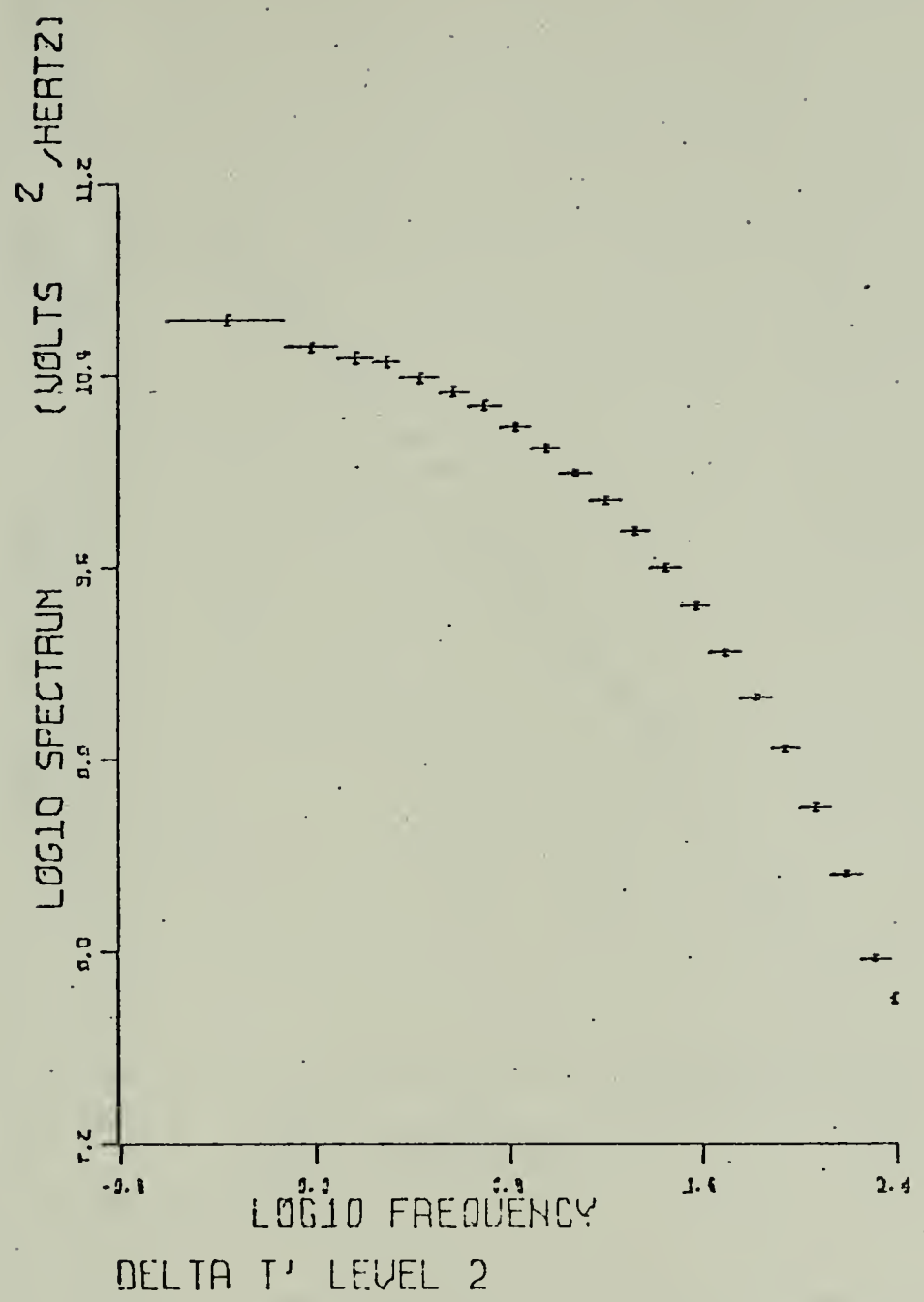

Figure 23. Differential Temperature Spectrum for Fluctuating Temperature Data Separated by r = 10 cm, Level 2 for 1855-1913, 18 Jan 74.

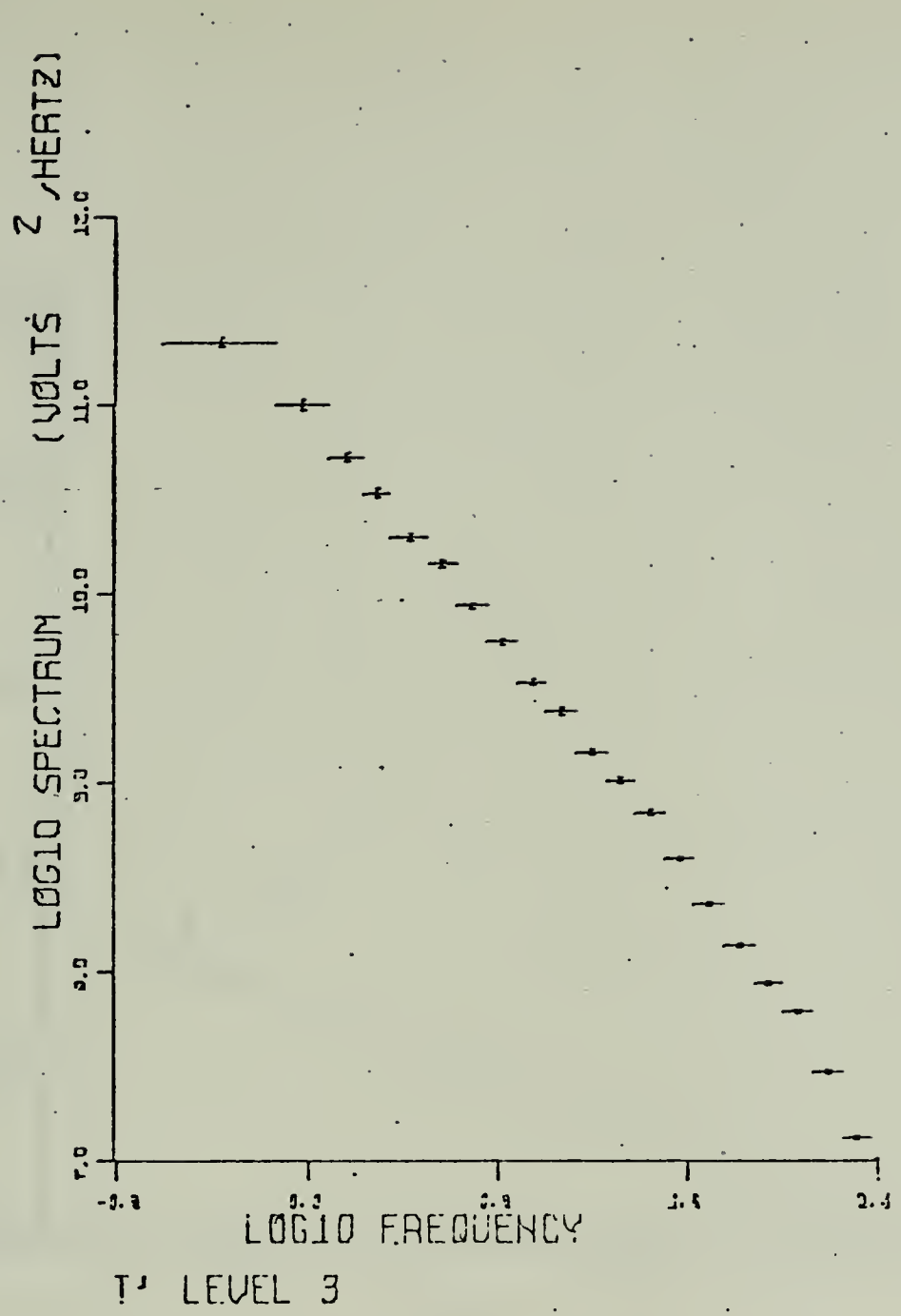

Figure 24. Temperature Spectrum Level 3 for 1855-1913, 18 Jan 74.

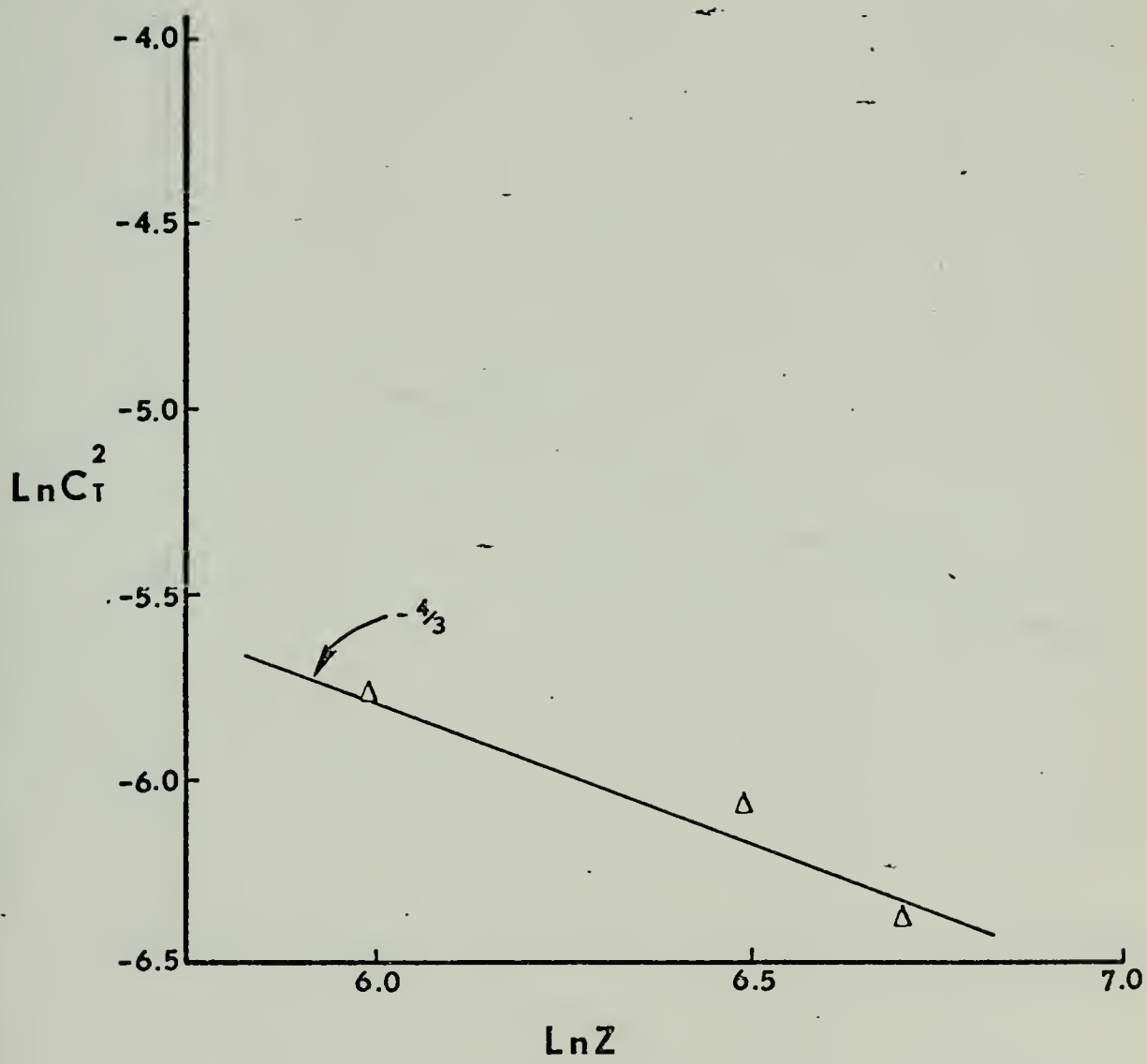

Figure 25. Measured Values of C_T^2 vs. Height for 1834-1854 18 Jan 74.

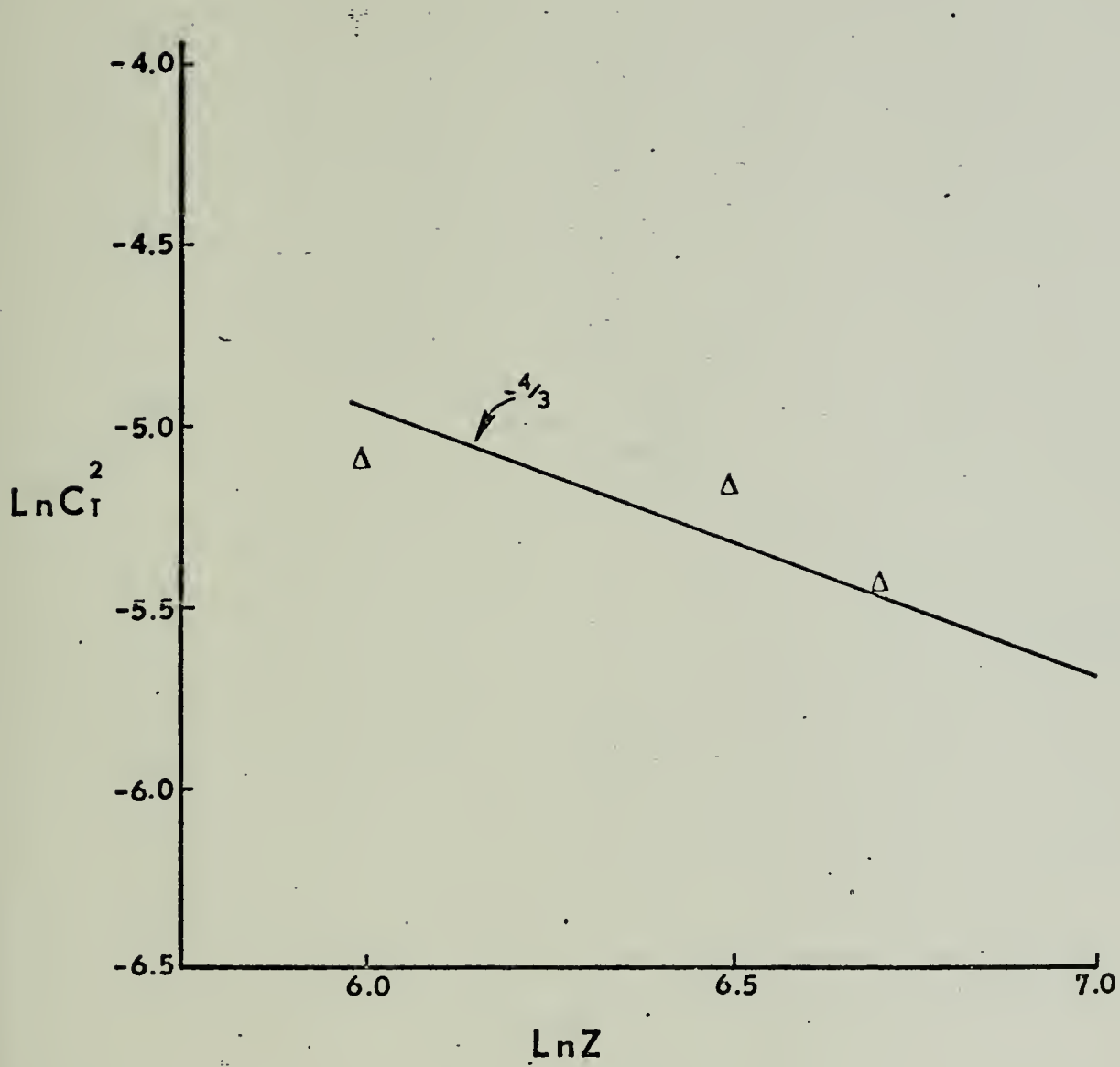

Figure 26. Measured Values of C_T^2 vs. Height for 1855-1913, 18 Jan 74.

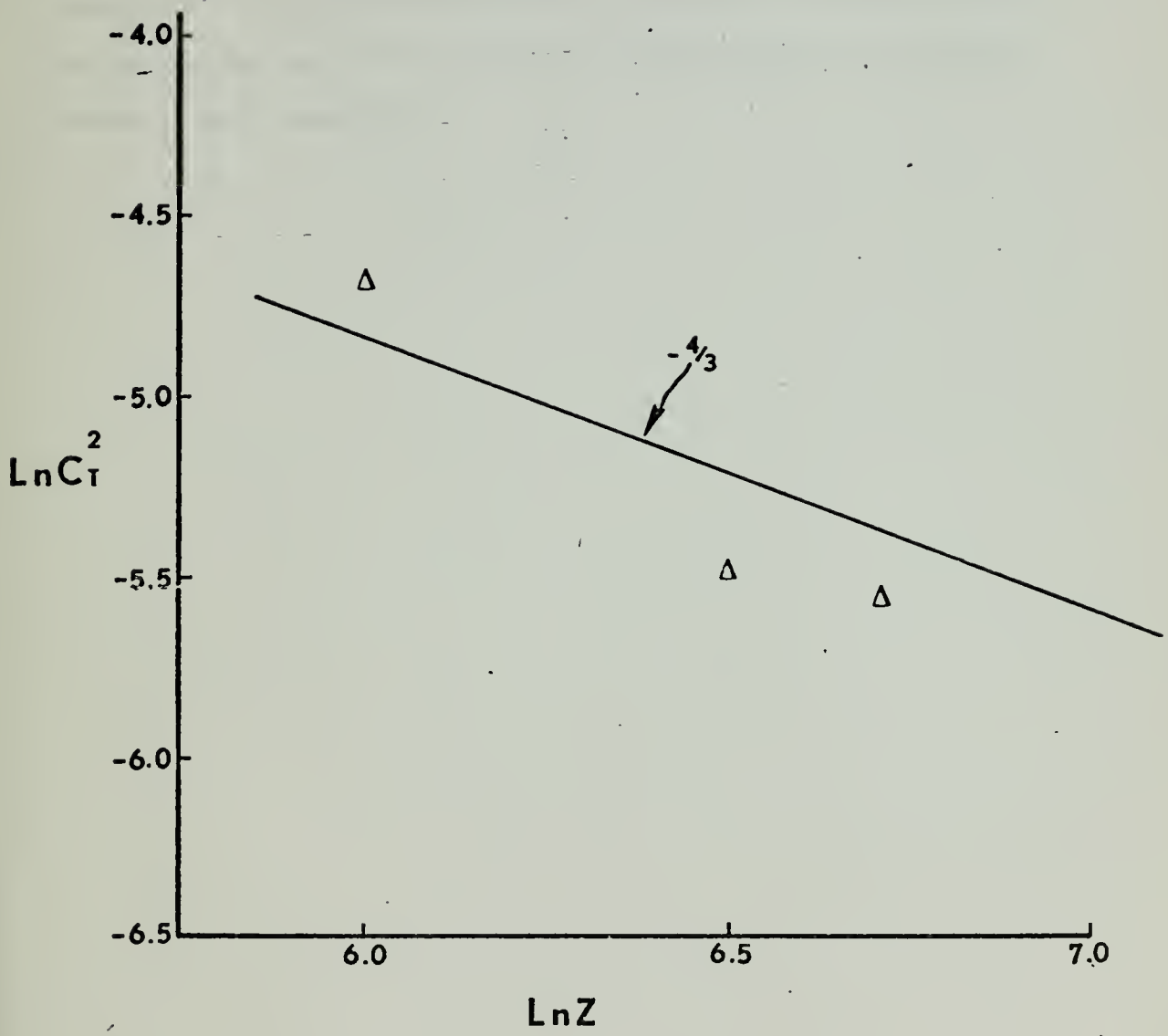

Figure 27. Measured Values of C_T^2 vs. Height for 1914-1932 18 Jan 74.

The above results give further support to the consideration that the bending is actual and not a result of random errors within the system, since these spectra were obtained from two independent sources, velocity and temperature measurements. However, no further explanation as to the cause of the bending is offered due to the limited amount of data considered.

VII. CONCLUSIONS AND RECOMMENDATIONS

Observed height variations of ε and C_T^2 tend to support present formulations and prediction techniques. However, several exceptions were noted and will be summarized in the following paragraphs.

For unstable atmospheric conditions slopes of $\ln \varepsilon$ versus $\ln Z$ were greater than -1. When these slopes were corrected for stability, there was a tendency for the slopes to shift towards a -1 slope. The observation was made that complete adjustment to a -1 slope was not evident, suggesting other factors such as wind wave effects may be important in near-ocean boundary theory. The observation was also made that $\ln \varepsilon$ versus $\ln Z$ was not a linear plot. There appeared to be bending or "kinking" which is not predicted in present formulations. No definite reason was given to account for the apparent kinking due to the limited amount of data examined.

A plot of $\ln C_T^2$ versus $\ln Z$ resulted in -4/3 slopes for unstable conditions. Some slight deviations were noted and attributed to other factors mentioned in the previous paragraph. The characteristic "kinking" or bending in the $\ln C_T^2$ versus $\ln Z$ plots was also evident.

Spectral analysis appears to be a satisfactory method for determining ε, momentum flux and C_T^2 estimates over the ocean. However, digital methods used are very time consuming due to the amount of tape handling and large computer programs used in spectral analysis. A real-time spectrum analyzer would increase the amount of data that one could examine due to the time saved in the analysis. It is suggested that

subsequent fluctuating velocity and temperature experiments aboard the ACANIA be examined using a spectrum analyzer in the analysis process.

LIST OF REFERENCES

1. Cardone, V. J., 1969: Specification of the wind distribution in the marine boundary layer for wave forecasting. New York University, School of Engineering and Science, Scientific Report GSL-TR69-1, University Heights, New York.

2. Johnston, W. E., 1974: Estimating boundary layer fluxes from shipboard measurements of dissipation of turbulent kinetic energy and temperature variance. M. S. Thesis, Naval Postgraduate School, Monterey, California, 131 pp.

3. Lumley, J. L., and Panofsky, H. A., 1964: The Structure of Atmospheric Turbulence, Interscience, New York, 239 pp.

4. McKendrick, J. M., 1972: An investigation of digital spectral analysis programs and computer methods utilized at the Naval Postgraduate School in the analysis of high frequency random signals. M. S. Thesis, Naval Postgraduate School, Monterey, California, 147 pp.

5. Paulson, C. A., 1970: "The mathematical representation of wind and temperature profiles in the unstable surface layer." J. Appl. Meteor., 9, 857-861.

6. Taylor, G. I., 1938: The spectrum of turbulence. Proc. Roy. Soc., A164, 476.

7. Tennekes, H., and Lumley, J. L., 1972: A First Course in Turbulence. MIT Press, 300 pp.

8. Welsh, P. T., 1974: An investigation of ship related motion and its effect on turbulence measurements. M. S. Thesis, Naval Postgraduate School, Monterey, California, 108 pp.

9. Wyngaard, J. C., Izumi, U., and Collins, S. A., 1971: "Behavior of the refractive-index-structure-parameter near the ground." Journal of the Optical Society of America, vol. 61, no. 12, 1646-1650.

INITIAL DISTRIBUTION LIST

		No. Copies
1.	Defense Documentation Center Cameron Station Alexandria, Virginia 22314	2
2.	Library (Code 0212) Naval Postgraduate School Monterey, California 93940	2
3.	Naval Oceanographic Office Library (Code 3330) Washington, D. C. 20373	1
4.	Commander, Naval Weather Service Command Naval Weather Service Headquarters Washington Navy Yard Washington, D. C. 20374	1
5.	Professor Kenneth L. Davidson, Code 51Ds Department of Meteorology Naval Postgraduate School Monterey, California 93940	13
6.	Professor Thomas M. Houlihan, Code 59Hm Department of Mechanical Engineering Naval Postgraduate School Monterey, California 93940	3
7.	Mr. P. Vial, Code 048 Naval Ordnance Laboratory White Oak Silver Spring, Maryland 20910	1
8.	Mr. B. Katz, Code 213 Naval Ordnance Laboratory White Oak Silver Spring, Maryland 20910	1
9.	Lieutenant Theron C. Bone 482 Alexis Ct. Marina, California 93933	1
10.	Mr. Steve Rinard, Code 51SR Department of Meteorology Naval Postgraduate School Monterey, California 93940	1

11.	Mr. Robert Smith Department of Research Naval Postgraduate School Monterey, California 93940	1
12.	Professor Dale F. Leipper, Code 58Lr Chairman, Department of Meteorology Naval Postgraduate School Monterey, California 93940	1
13.	R/V ACANIA Department of Oceanography Naval Postgraduate School Monterey, California 93940	1
14.	Dr. P. Livingston Applied Optics Branch, Bldg. 30 Naval Research Laboratory Washington, D. C.	1

Thesis
B6796 Bone
c.1
155028
Small scale properties
in the marine boundary
layer.